Copyright

By

Ramadevi Duraisamy

2005

Finite Element Study of Mast Arm Socket Welded Connections

by

Ramadevi Duraisamy, B.E.

Thesis

Presented to the Faculty of the Graduate School of

The University of Texas at Austin

in Partial Fulfillment

of the Requirements

for the Degree of

Master of Science in Engineering

The University of Texas at Austin

December 2005

Finite Element Study of Mast Arm Socket Welded Connections

APPROVED BY
SUPERVISING COMMITTEE:

Karl H. Frank

Loukas F. Kallivokas

Dedication

To my lovable family and friends

Acknowledgements

I wish to express my profound gratitude to my advisor Dr. Karl H. Frank for his guidance and support throughout my research. His affability and continuous encouragement throughout my work helped me in completing my research work successfully well before the stipulated time.

I would like to extend my gratitude to Dr. Loukas F. Kallivokas for his patience and valuable suggestions for this thesis.

I would also like to thank manager and staff of Civil Engineering Learning Resource Center (CE-LRC) for their continuous support and help towards my analytical study using Abaqus software.

Finally, I would like to thank God for giving me this golden opportunity to work on this project and hone my research skills

December 2005

Finite Element Study of Mast Arm Socket Welded Connections

Ramadevi Duraisamy, M.S.E.

The University of Texas at Austin, 2005

SUPERVISOR: Karl H. Frank

There has been a rise in the number of failures of traffic cantilever signal mast arms in recent years due to increasing spans of mast arms and the inherent flexibility of the structures. This increased flexibility makes mast arm socket welded connections more critical.

Extensive finite element analysis using Abaqus was carried out in this study to determine the effect of different geometric variables like end plate thickness, mast arm diameter, mast arm thickness and weld geometry on stress at the weld toe by estimating the Stress Concentration Factor (SCF) at weld toe. Two different approaches, Dong's Structural Stress and Det Norske Veritas (DNV), were used to calculate the SCF at weld toe. To study the effect of end plate thickness, six models with different end plate thicknesses were analyzed. Effect of geometric variables like mast arm thickness, mast arm diameter, and

weld geometry were studied for all the six different end plate thicknesses. It was found that of all of the geometric variables analyzed, end plate thickness had a greater effect on stresses at weld toe.

Experimental results of fatigue behavior of mast arms socket welded connections from other research projects were used to investigate the hypothesis which states that, fatigue life (N) is some constant (A) times the stress range (SCF x S_R) raised to the third power, where the constant (A) is the fatigue life coefficient. Investigation of the above stated hypothesis was done using both approaches for calculating SCF, namely Dong's Structural Stress and DNV. From hypothesis investigation, it was found that scatter in the experimental data is reduced when maximum stress range at weld toe (SCF x nominal stress range) is plotted against fatigue life as compared to plotting nominal stress range against fatigue life.

Table of Contents

CHAPTER 1 INTRODUCTION 1

1.1 Background 1

1.2 Project Scope 5

CHAPTER 2 LITERATURE REVIEW 7

2.1 Cantilever mast arm traffic signal structure 7

2.2 Wind load effects 9

2.2.1 Natural Wind Gusts 9

2.2.2 Truck Induced Wind Gusts 10

2.2.3 Vortex Shedding 12

2.2.4 Galloping 13

2.3 Failures of Traffic Signal Mast Arms 16

2.4 Related research 17

CHAPTER 3 FINITE ELEMENT MODELING 19

3.1 Introduction 19

3.2 Analysis tools and techniques 19

3.3 Stress Concentration Factor calculation (SCF) 21

3.3.1 DNV Technique 22

3.3.2 Structural Stress Technique 23

3.4 Convergence Study 26

CHAPTER 4 ANALYSIS RESULTS 31

4.1 Introduction 31

4.2 Effect of geometric variables on SCF 31

4.2.1 End plate thickness 31

4.2.2 Mast Arm outer diameter 35

4.2 Hypothesis investigation 41

CHAPTER 5 CONCLUSIONS AND RECOMMENDED RESEARCH 47

5.1 Conclusions……. 47

5.2 Recommendations for Future Research 49

APPENDIX A 50

APPENDIX B 52

APPENDIX C 63

APPENDIX D 67

REFERENCES 68

VITA. 69

List of Figures

Figure 1.1 Typical Cantilever Mast Arm Traffic Signal Support Structure..... 2
Figure 1.2 Traffic signal structure failure in Pflugerville [11]..... 3
Figure 1.3 Failure due to fatigue crack initiated at top of mast arm [11]..... 4
Figure 1.4 Failure of traffic signal mast arm in Wyoming [7]..... 4
Figure 1.5 Failure due to fracture at the connection between mast arm and the pole connected to the foundation in Wyoming [7]..... 5
Figure 2.1 Typical Mast Arm Built-Up-Box Connection detail 7
Figure 2.2 Fillet Welded Socket Connection detail 8
Figure 2.3Truck passing under Variable Message Signs [6] 11
Figure 2.4 Vortex Shedding in a Mast [6]..... 12
Figure 2.5 Galloping [6]..... 14
Figure 3.1 Solid Symmetric Model..... 20
Figure 3.2 Fine Mesh……21
Figure 3.3 Coarse Mesh 21
Figure 3.4 Stress Extrapolation 23
Figure 3.5 Structural stresses definition for through thickness fatigue crack. (a) Local through-thickness normal and shear stress at weld toe, (b) Structural stress definition at weld toe [5]..... 24
Figure 3.6 Structural stresses calculation procedure for through-thickness fatigue crack [5]..... 25
Figure 3.7 Two different geometries with end plate thickness = 1.5 inches used for convergence study 26
Figure 3.8 Mesh Convergence study using Dong's Structural Approach..... 28

Figure 4. 1 Mast Arm End plate geometry used for studying effect of End plate thickness on SCF 32
Figure 4. 2 Effect of End plate thickness-Comparison of DNV and DONG's Approaches 33
Figure 4. 3 % reduction in SCF relative to 1 in thick plate using DONG's approach 34
Figure 4. 4 % reduction in SCF relative to 1 in thick plate using DNV approach 34
Figure 4. 5 Front Elevation showing Mast Arm base outer diameter 35
Figure 4. 6 6.5" and 11" Mast Arm base outer diameter 36
Figure 4. 7 Effect of Mast Arm Outer Diameter on SCF for different End plate thicknesses using DNV Approach..... 37
Figure 4. 8 Effect of Mast Arm Outer Diameter on SCF using DONG's Approach 38
Figure 4. 9 Effect of Mast Arm Outer Diameter on SCF using DNV Approach.. 38
Figure 4. 10 TXDOT specifications for Arm Base Weld details 39
Figure 4. 11 Effect of Weld Geometry for different End plate thicknesses using DNV Approach..... 40
Figure 4. 12 Effect of Weld Orientation on Maximum Principal Stress along Mast Arm Length 41
Figure 4. 13 Hypothesis investigation using DONG's Approach..... 45
Figure 4. 14 Hypothesis investigation using DNV Approach..... 46
Appendix A- 1 Mast Arm – End plate geometry used……...50

List of Tables

Table 3.1 Abaqus Material Properties 20
Table 3.2 Dong's Structural Stress Approach-Specimen 'A' 27
Table 3.3 Dong's Structural Stress Approach-Specimen 'B' 27
Table 3.4 DNV Approach-Specimen 'A' 29
Table 3.5 DNV Approach-Specimen 'B' 29
Table 4. 1 Analyzed Models 42
Table 4. 2 Stress Concentration Factor using DONG's Approach 43
Table 4. 3 Stress Concentration Factor using DNV Approach 43
Table 4. 4 S-N values obtained using two approaches 44
Table 4. 5 Hypothesis Investigation Results 46
Table A- 1 DNV Approach 51
Table A- 2 Dong's Structural Stress Approach 51
Table B- 1 Abaqus analysis results for Mesh Convergence study using DNV approach-Specimen 'A' 52
Table B- 2 Abaqus analysis results for Mesh Convergence study using DNV approach-Specimen 'B' 53
Table B- 3 Abaqus analysis results for TXu specimen 54
Table B- 4 Abaqus analysis results for VALu specimen 55
Table B- 5 Abaqus analysis results for VALNu specimen 56
Table B- 6 Abaqus analysis results for VALNu2 specimen 57
Table B- 7 Abaqus analysis results for Nippon Steel A specimen 58
Table B- 8 Abaqus analysis results for Nippon Steel B specimen 59
Table B- 9 Abaqus analysis results for the study investigating effect of end plate thickness and mast arm outer diameter on SCF at weld toe-11 in mast arm diameter 60
Table B- 10 Abaqus analysis results for the study investigating effect of mast arm outer diameter on SCF at weld toe – 6.5 in mast arm diameter 61

Table B- 11 Abaqus analysis results for the study investigating the effect of weld dimensions on SCF at weld toe – 7g weld for 0.179 thick mast arm……62
Table C- 1 Abaqus analysis results for the study investigating the effect of weld orientation on stresses at weld toe…….63
Table D- 1 Abaqus analysis results for Mesh Convergence study using DONG's Structural Stress approach-Specimen 'A'……. 64
Table D- 2 Abaqus analysis results for Mesh Convergence study using DONG's Structural Stress approach-Specimen 'B'……..65
Table D- 3 Abaqus analysis results for TXu and VALu specimens……..65
Table D- 4 Abaqus analysis results for VALNu and VALNu2 specimens……...66
Table D- 5 Abaqus analysis results for Nippon steel specimens……...66
Table D- 6 Abaqus analysis results for the study investigating effect of end plate thickness and mast arm outer diameter on SCF at weld toe – 11 in mast arm diameter……..67
Table D- 7 Abaqus analysis results for the study investigating effect of end plate thickness and mast arm outer diameter on SCF at weld toe – 6.5 in mast arm diameter……..67

CHAPTER 1
Introduction

1.1 BACKGROUND

This study investigated the effect of the various geometric variables on stresses at socket welded connections of cantilevered traffic signal mast arms (Figure 1.1) to estimate their influence upon fatigue performance of these structures. Traffic signal structures in U.S. are described based on the types of vertical and horizontal members. Vertical members are referred to as columns, poles, posts or masts (Figure 1.1). Traffic signal structures with only one pole or column are referred to as cantilever structures based on the cantilevered horizontal member. Sign bridge or overhead structures are ones with two or more columns. The horizontal member consisting of one member is called a monotube or mast-arm (Figure 1.1) and usually consists of a tapered tube in order to reduce the dead load of the structure. Another type of horizontal member is one which consists of a truss and the truss structure usually has two chords and is called a two-chord truss. Cable structure is another commonly used traffic signal structure, which is different from the above categories, and has series of cables to support the traffic signal.

The single column structure (Figure 1.1) has many advantages over other structures such as fewer collision hazards and vision obstacles for drivers, cost effectiveness, simple design, and good aesthetic appearance. However it is a non-redundant structure which is discussed in detail in chapter 2. Report by Dexter indicated that the number of failures of traffic signal mast-arms has increased in the recent years [2]. This increase can be attributed to the increasing spans of

mast-arms due to widening of roadways across U.S. to increase the traffic capacity. The low natural frequencies associated with these lightweight and long span flexible structures makes them more susceptible to resonance, which can lead to a large number of relatively high stress cycles. Thus the flexibility, combined with the lengths of mast-arms utilized today makes them more prone to fatigue problems. Geometry of the two chord truss structures and multicolumn structures eliminates many of the vibrations that lead to the high numbers of stress cycles.

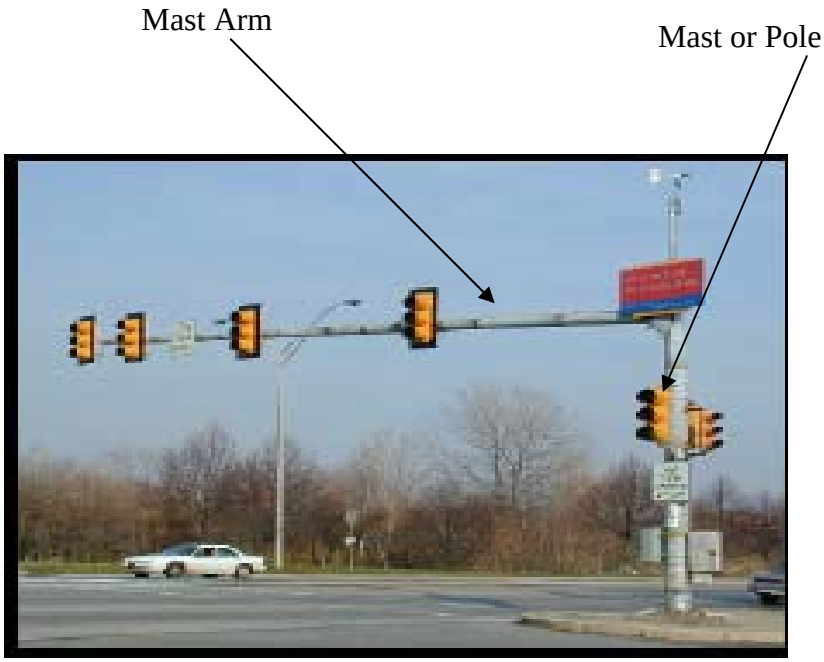

Figure 1.1 Typical Cantilever Mast Arm Traffic Signal Support Structure [15]

In a typical cantilever mast-arm structure, the connection details at the mast-arm to column connection and the column to base plate connection are identical, which creates two possible critical locations. But, the column has a larger cross section, which helps in reducing the local stresses at the column to base plate connection. Also, the column is under compressive force, which further

reduces the local tensile stresses at the column to base plate connection. The above mentioned factors make mast-arm to column connection to be the critical connection and hence mast-arm to column connection is considered in this study.

Increasing occurrences of fatigue cracking experienced by many state departments of transportation and urban municipalities has lead to considerable amount of research interest related to fatigue performance of cantilevered sign structures. Figure 1.2 and Figure 1.3 show the Pflugerville failure in the state of Texas. The collapse of a traffic signal pole in Wyoming is shown in Figure 1.4 and Figure 1.5. Failure of this structure at Wyoming is not under an extreme wind event [7]. Vibrations at lower wind speeds most likely caused the fatigue initiation and subsequent crack growth. The collapse was the result of a fracture at the connection between the mast arm and the pole connected to the foundation.

Figure 1.2 Traffic signal structure failure in Pflugerville [11]

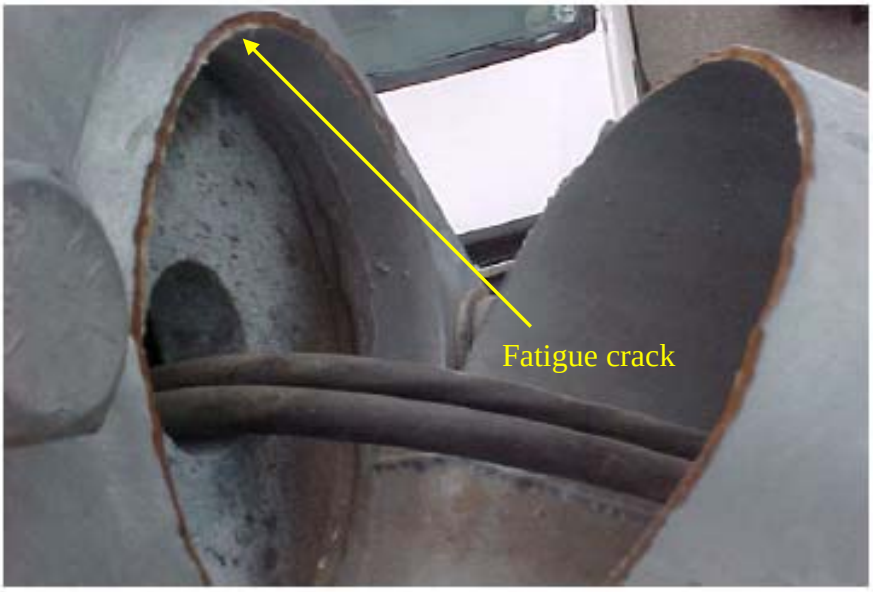

Figure 1.3 Failure due to fatigue crack initiated at top of mast arm [11]

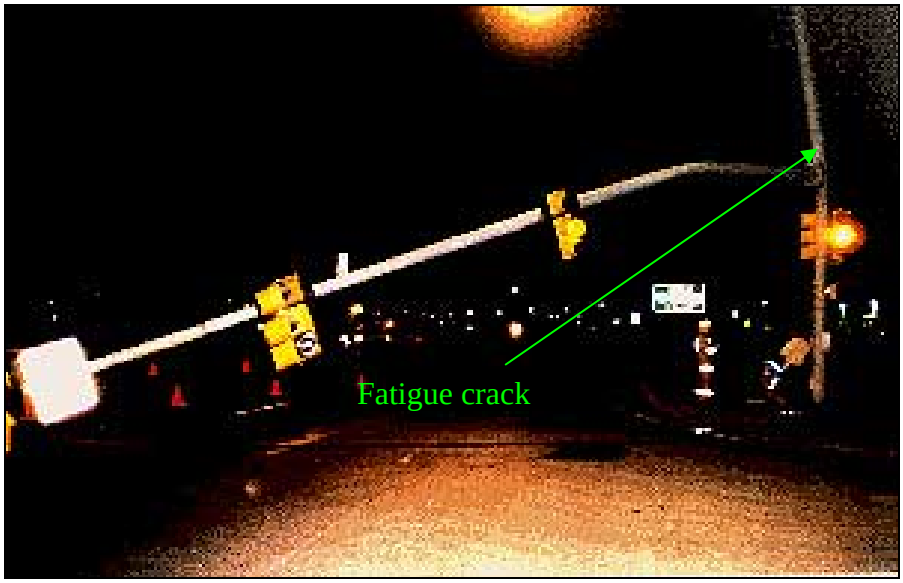

Figure 1.4 Failure of traffic signal mast arm in Wyoming [7]

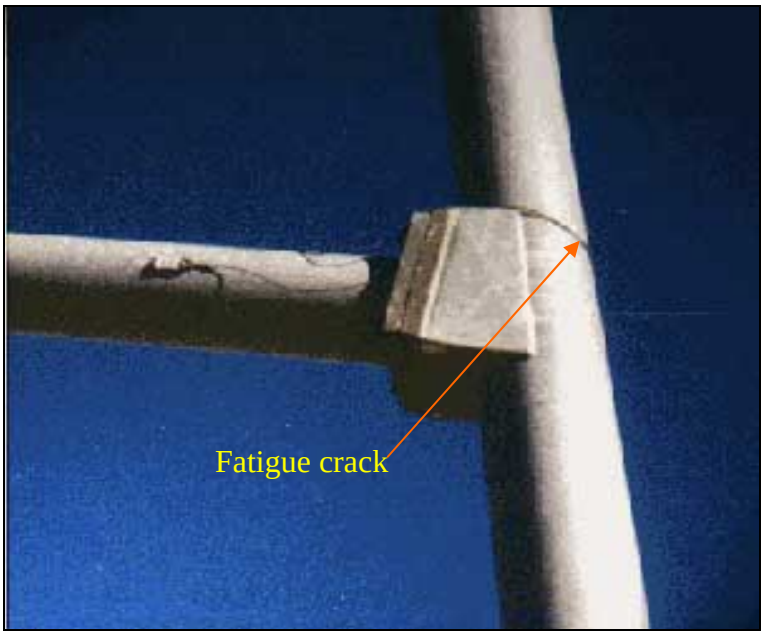

Figure 1.5 Failure due to fracture at the connection between mast arm and the pole connected to the foundation in Wyoming [7]

The influence of connection geometry and mast arm size was investigated with the goal of providing the designer with ability to size the connection to enhance its fatigue performance.

1.2 PROJECT SCOPE

In this study, effect of different geometric variables like base plate thickness, mast arm diameter, mast arm thickness and weld geometry on stress at the weld toe is studied by estimating the Stress Concentration Factor (SCF) at weld toe. Two different approaches Dong's Structural Stress approach and Det Norske Veritas (DNV) are used to calculate the Stress Concentration Factor (SCF) at weld toe. These two approaches are discussed in chapter 2. To study the

effect of base plate thickness, six models with different base plate thicknesses were analyzed. One interesting aspect of this research is that the effects of geometric variables like mast arm thickness, mast arm diameter, and weld geometry were studied for six different base plate thicknesses. This is done as base plate flexibility, compared to other geometric variables, has been found to have a greater effect on stresses at weld toe from earlier study [12], [4] and from this project. The results are discussed in chapter 4.

Experimental results from other research projects [1], [4] were used to investigate the hypothesis which states that, fatigue life (N) is some constant (A) times the stress range (SCF x S_R) raised to the power three, where the constant (A) is the Fatigue life coefficient. Results of hypothesis investigation are discussed in chapter 4. General conclusions from the test results, as well as recommendations for further research are presented in chapter 5.

CHAPTER 2
Literature Review

2.1 CANTILEVER MAST ARM TRAFFIC SIGNAL STRUCTURE

This study focuses on the mast arm to column (pole or mast) connection. Figure 2.1 shows a close-up view of a typical mast arm to column connection. The tapered tube of mast arm is connected to the end plate with a fillet-welded socket connection. The end plate is in turn connected to the built-up box.

Figure 2.1 Typical Mast Arm Built-Up-Box Connection detail

The end plate is cut-out to allow the mast arm to fit inside it and hence the name socket connection. Figure 2.2 shows the fillet welded socket connection

detail. As can be seen from the figure, the tapered tube of the mast-arm is socketed into a hole through the end plate. The end plate and the tube are then connected by two fillet welds. The primary weld is a multiple pass unequal leg fillet weld located on the outside of the tube. This weld transfers the majority of the forces from the tube to the end plate. The second weld is a small fillet weld connecting the end of the tube to the inside of the end plate hole. Primary function of this secondary weld is to seal the connection to prevent corrosion and entrance of molten zinc during galvanizing. Experimental studies show that the secondary weld does not transfer a significant amount of load [1].

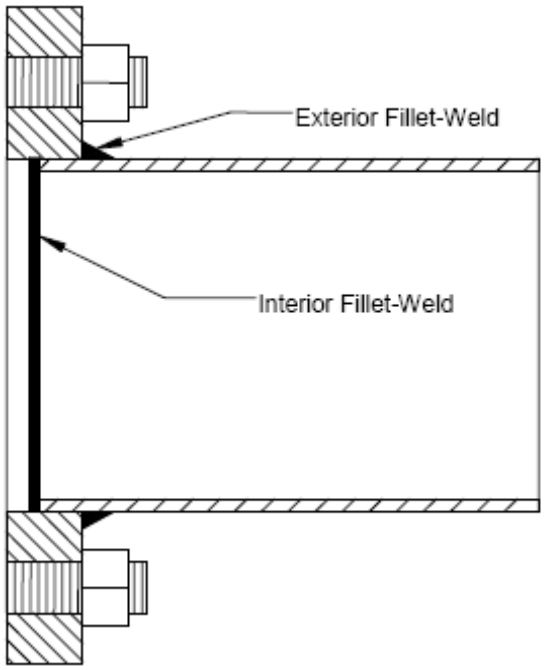

Figure 2.2 Fillet Welded Socket Connection detail

The hole cut out into the end plate allows the drainage of the molten zinc from the interior of the arm during the galvanizing process. However, this hole significantly reduces the bending stiffness of the end plate. Failure occurs when

there is cracking at the toe of the fillet weld connecting the end plate to the arm. This cracking may be caused by the repeated fatigue stresses produced by movement of the mast arm from ambient wind or gusts from trucks passing under the signal.

2.2 WIND LOAD EFFECTS

The extent of the vibrations of the traffic signal mast arms under service conditions, resulting in fatigue related problems was studied and documented by Kaczinski et al. (1998). Four wind phenomena namely natural wind gusts, truck induced wind gusts, vortex shedding, or galloping can cause the vibrations of traffic signal mast arms. The wind phenomena have been investigated by research conducted at the University of Minnesota, the University of Florida, the University of Wyoming, and Texas Tech University [1].

2.2.1 Natural Wind Gusts

The most common type of wind-induced vibration in support structures is from ordinary wind gusts or fluctuations of the wind velocity [6]. In the 2001 AASHTO (American Association of State Highway and Transportation Officials) Specifications, these gusts are referred to as natural wind gusts to distinguish them from truck-induced wind gusts. Also, in the 2001 AAHSTO Specifications, the natural wind gust pressure is applied horizontally to the projected frontal area of all surfaces, including the structural members, as well as the sign and signal attachments.

Cracking developed over a period of at least several years in cases where fatigue cracking was caused by natural wind gusts. In cantilevered sign and signal support structures, the cracks will usually manifest at the connection of the mast arm to the pole, with cracks forming along the sides of the connection [6]. Support structures in certain areas of the country that are very windy are

particularly susceptible to vibration and fatigue from natural wind gusts [6]. Typically, these are places where the mean annual wind velocity is greater than 5 m/s (10 mph). These places where there are frequent constant winds, and support structures are at risk for fatigue cracking due to natural wind gust loading, are different from the same places with the maximum peak wind velocities that are identified on wind maps, such as those in ASCE 7-98. These maps show the maximum wind speed that occurs over a 50-year period that is used for strength design.

The fatigue-limit-state natural wind gust loads in the 2001 AASHTO Specifications are derived for winds that are exceeded about 2 hours each year. Such areas are not necessarily those with occasional very high winds such as hurricanes or tornadoes. For example, the four places in the United States with the greatest wind velocities that are exceeded at least 2 hours per year are [6]:

- Tatoosh Island, Washington: 28 m/s (62 mph)
- Clayton, New Mexico: 24 m/s (53 mph)
- Point Judith, Rhode Island: 24 m/s (53 mph)
- Cheyenne, Wyoming: 24 m/s (53 mph)

2.2.2 Truck Induced Wind Gusts

The passage of trucks beneath support structures induces both horizontal and vertical gust loads on the structure, creating a motion that is primarily vertical but may also include a significant horizontal component as well. In the specifications, horizontal truck gust is neglected as the magnitude of the horizontal truck gust is negligible relative to the natural wind gust. The vertical truck gust load in the specifications is an equivalent static pressure range applied to the underside of the mast arm or truss and any attachments. Due to the large depth of variable-message signs (VMS) in the direction of traffic flow (up to 1.2

m for older signs), the support structures are the most susceptible to truck-induced wind gust fatigue, as seen in Figure 2.3.

Figure 2.3Truck passing under Variable Message Signs [6]

Fatigue cracking from truck-induced wind gusts usually develops over a period of several years. However, one case of a failure of a cantilever VMS structure, reported by DeSantis and Haig, was to a structure less than 1 year old. The cracks will usually manifest at the connection of the mast arm to the pole, at truss connections; and at the base of the pole to the weld joining the pole to the end plate, at the top of the stiffeners, at hand holes, or at the anchor rods [6].

As the truck-gust pressure is proportional to the speed of the trucks, signs located on major highways are more susceptible than those where the trucks are traveling slowly. There is a vertical gradient for the truck-induced gust pressure, so the greater the clearance between the tops of trucks and the bottoms of the

signs, the less the susceptibility to truck-induced vibration. The truck-gust loads essentially go to zero at a height of 10 m (32.8 ft) above the roadway.

2.2.3 Vortex Shedding

Vortex shedding is the shedding of vortices on alternate sides of a symmetric member (i.e., one without any attachments). Vortex shedding can result in resonant oscillations of a pole in a plane normal to the direction of wind flow as shown in Figure 2.4 [6]. In the 2001 AASHTO Specifications, the vortex shedding pressure range for fatigue design is applied horizontally and vertically to the projected area of one side of the mast and mast arm respectively to calculate the fatigue stress ranges in the details.

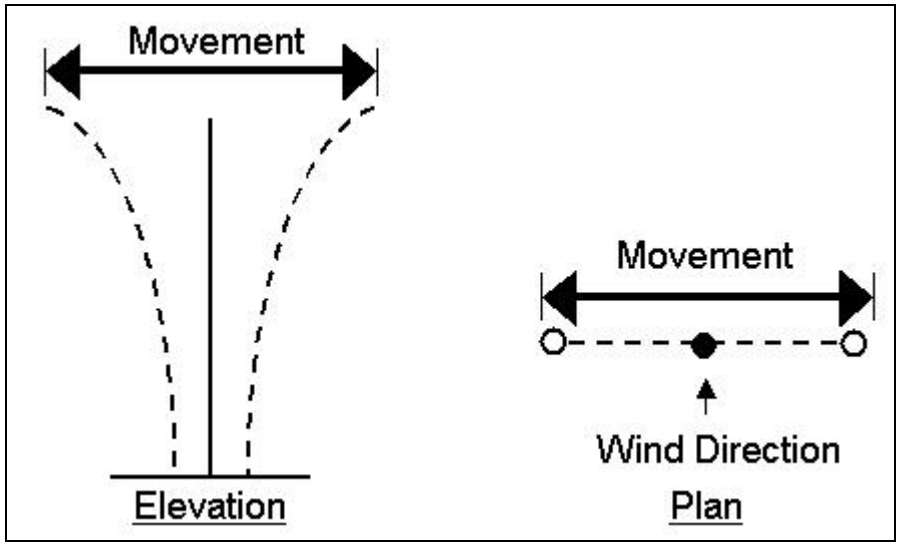

Figure 2.4 Vortex Shedding in a Mast [6]

The vortices are shed in an alternating pattern that is known as a Von Karman vortex street. If the frequency of the shedding of the vortices approaches one of the natural frequencies of the structure, a condition called lock-in may develop. Under lock-in, the displacement of the mast arm induces a stronger, more regular vortex shedding pattern, which in turn leads to larger displacements. In this manner, if lock-in occurs, the vortex shedding may cause significant displacements at the tips of mast arms and significant stress ranges at the critical connection details [1].

Using Strouhal relation of fluid mechanics, the potential for lock-in of a structure may be calculated. The Strouhal relation states that the frequency of vortex shedding is dependant on the wind velocity and across-wind dimension of the structure, or the diameter of a mast arm. In the case of a tapered mast arm, under a given wind condition, the changing diameter limits the length of lock-in to only a small portion of the overall structure [1]. The loading of the small regions for which lock-in may occur is typically too small to create significant oscillations of the entire structure.

The traffic signal attachments have also been shown to not be susceptible to vortex shedding lock-in, however signs may be susceptible (Kaczinski, 1998). If lock-in occurs on a sign, the loading may be substantial enough to initiate galloping, the fourth wind phenomenon.

2.2.4 Galloping

Galloping is different than vortex shedding but also results in large-amplitude, resonant oscillations perpendicular to the direction of wind flow as shown in Figure 2.5. Unlike vortex shedding, galloping occurs on asymmetric members (i.e., those with signs, signals, or other attachments) rather than circular members. Therefore, it is the mast arms rather than the poles that are susceptible

to galloping. Galloping has caused mast arms to move up and down with a range greater than 1 m. According to NCHRP Report 469, a large portion of the vibration and fatigue problems that have been investigated for cantilevered sign and signal support structures were caused by galloping.

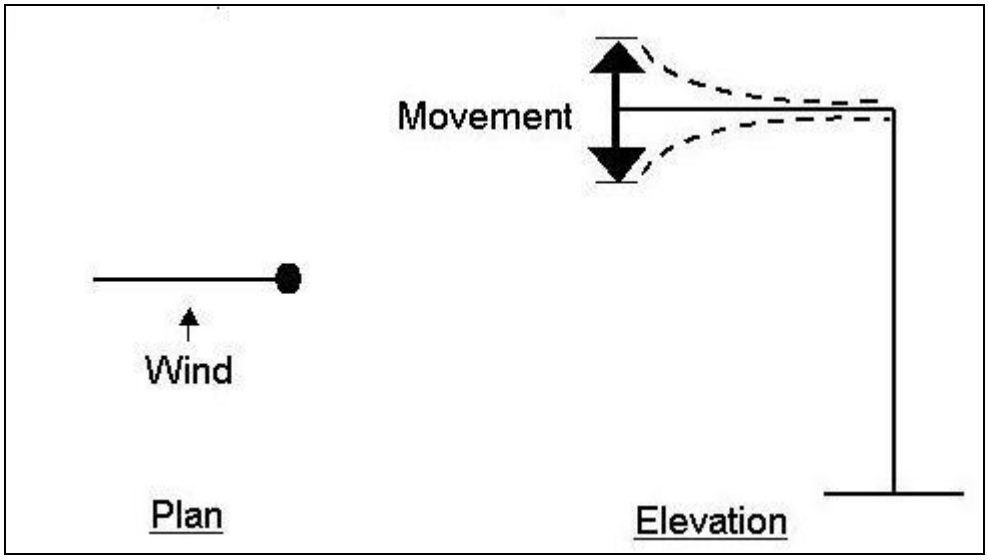

Figure 2.5 Galloping [6]

Attachments like signs/signals cause galloping. The number of signs and signal heads, their configuration, area, connection detail, and the direction of wind flow significantly influence the susceptibility for galloping [6]. Signal attachments configured with back plates and subjected to flow from the rear are most susceptible to galloping [6], [1]. However, all types of signal heads and signs have been observed to be affected by galloping, even those with louvered back plates.

Galloping also requires uniform steady winds rather than gusty winds. However, in contrast to vortex shedding, galloping can continue over a large range in wind velocity [6]. The mode of vibration for galloping is displacement of

the mast arm in the vertical direction. This mode typically has a frequency closer to 1 Hz (1 second period). Higher modes of vibration have not been observed. Consequently, flexible monotube cantilever support structures are particularly susceptible to galloping.

The galloping loads are quite severe, so when they are applicable, they will typically govern the fatigue design. Therefore, mitigation devices will have significant cost benefits in reducing the effects of galloping. In most cases that have been investigated, the fatigue cracking that has occurred from galloping has developed over a long period of a year or more where there may have been many days of winds that caused galloping. In cantilevered sign and signal support structures, the cracks will usually manifest at the connection of the mast arm to the pole or at the base of the pole. In truss mast arms, the cracks may form at the truss connections, usually those closest to the pole. If there is a flanged splice detail in the mast arm close to the pole, this may also be a critical location where cracks may form. At the base of the pole, cracks may form at the weld joining the pole to the end plate [6]. If there are stiffeners or gussets reinforcing the pole to end plate connection, then the cracks will typically form at the tops of the stiffeners. If there are hand holes, cracks may appear around the perimeter of these. Cracked anchor rods have also occurred.

The potential susceptibility of a structure to galloping can be calculated based on an equation called the Den Hartog stability criterion [3]. The Den Hartog stability criterion states that a structure is susceptible to galloping if the summation of the structure's lift force coefficient and the drag coefficient produces a negative value. The wind velocity acting on a structure must also exceed a minimum onset velocity in order to initiate galloping behavior.

In the fatigue provisions of the 2001 AASHTO Highway Signs, Luminaries, and Traffic Signal Specifications, the forces due to galloping are

applied to the structure as a 21 psf pressure applied vertically to the surface area of any attachments on the structure. The 21 psf load was determined through wind tunnel testing on scale models [1]. However, this loading of the frontal areas of all attachments does not seem to account for the susceptibility of attachments with only specific geometries to experience galloping. This loading is an indirect method of applying loads to simulate the stresses caused by galloping. It is widely acknowledged that the galloping phenomenon is the most likely wind phenomenon to cause a large number of significant stress ranges at the critical sections of traffic signal mast arms, although the causes of and the loads associated with galloping may not be fully understood.

2.3 FAILURES OF TRAFFIC SIGNAL MAST ARMS

The design of cantilevered sign structures is typically controlled by fatigue. Fatigue is the likely cause of failure in cantilevered sign structures. This section provides a brief overview of fatigue. As mentioned in Chapter 1, cantilever mast arm traffic signal structure is a non-redundant structure and the mast arm is very flexible. The welded connections in these structures have no redundancy. Any visible sign of a fatigue crack noted during inspection requires the immediate replacement of the structure. The total fatigue life of a structure is the sum of initiation and propagation cycles [14]. Beginning of fracture marks the end of fatigue life. Fracture is the rapid extension of the crack in tension causing collapse. The magnitude of the fluctuating local stress at the stress raiser, stress pattern, the physical attributes of the structure, and the environment are the various factors affecting fatigue [12]. The fatigue resistance of welded details primarily depends on the nominal stress range and the notch severity [12]. Nominal stress refers to the calculated stress at the structural level neglecting the presence of geometrical stress concentration and welds. Notch severity includes

all of the effects for the practical range of structure configuration and welded geometry of the particular detail.

2.4 RELATED RESEARCH

The issue of fatigue in traffic signal mast arms was first studied at Lehigh University in 1983, and the effects of fatigue were first documented under service conditions in a survey performed by Kaczinski et al. in 1993. The results from the research conducted at Lehigh University indicated that the typical socket weld connection in use was worse than a category E' detail with an equal fillet weld, and the same connection was a category E detail with an unequal leg filled weld [1]. 55 full size mast arm connection detail specimens were tested for fatigue resistance at the University of Texas at Austin [13]. The results of this research project indicate that Ultrasonic Impact Treatment weld treatment can significantly improve the fatigue life of a fillet-welded socket connection detail. The test results of this research also confirmed the classification of the unequal leg fillet welded socket connection detail as an E' category detail. Several other connection details exhibited improved fatigue lives. An extensive finite element analysis which was part of this study generated stress concentration factors (SCF) for a variety of connection geometries. These finite element analyses extended the range of geometries beyond those included in the experimental study. In the experimental study only two specimens with thicker end plate specimens were studied. However, this was the first research work which showed that end plate thickness is an important factor affecting SCF at weld toe.

The effect of end plate flexibility on the stress behavior and hence fatigue performance of welded socket connections in cantilevered sign structures was studied at Lehigh University [13]. From this study it was found that end plate flexibility, primarily end plate thickness, has a drastic influence on the stress

behavior in the pole tube wall adjacent to the socket welded connection. This study also concluded that increasing end plate thickness drastically reduce stresses at the fatigue critical vertical weld toe. However, this study concentrated on the pole - end plate connection and not on the mast arm - end plate connection. Extensive finite element study to better understand the influence of end plate flexibility on the fatigue performance of socket welded connections in cantilevered sign structures formed part of this study.

Research was conducted at the University of Texas at Austin to investigate UIT (Ultrasonic Impact Treatment) as a viable retrofit for in-service traffic signal structures [4]. One of the suggestions of this research project is to treat both weld toes of mast arm-end plate fillet welded socket connection, as two of the tested specimens had crack initiation at the untreated end plate weld toe.

CHAPTER 3
Finite Element Modeling

3.1 INTRODUCTION

This section discusses the results of a study carried out to investigate the effect of mesh size upon the results. Also summarized in this section are the analysis tools and techniques used in creating, analyzing and evaluating the finite element models and results.

3.2 ANALYSIS TOOLS AND TECHNIQUES

Abaqus Standard v. 6.5 was used to analyze the mast arms on a Windows XP workstation with 3.39 GHz Intel Pentium Xeon processor, 1GB of RAM, and 36 GB of hard disk space. All analyses were performed statically. The finite element models were created by drawing solid symmetric models of test specimens using AutoCAD 2005. Earlier research [1] indicated that mast arm length has no influence on the socket weld SCF and test specimens used in the experimental study were of 90 inches-95 inches in length. Hence, length of the model used in this study is restricted to 90 inches. Since the model is symmetric, only half portion of the model was used for analysis as shown in Figure 3.1. To enable this, half the model was cut from the full symmetric model and exported from AutoCAD and imported into Abaqus as a deformable part. The entire arm was assigned steel as the material property except for a small 5 in length towards the mast arm end which was assigned rigid material to facilitate the application of concentrated load to the mast arm. This end rigid portion of Mast Arm was called as loading Plate as shown in Figure 3.1. Table 3.1 shows the elastic properties of

the materials. A 20-node quadratic solid (C3D20 in Abaqus) element was used in the mesh. Mesh size was arrived at after doing a convergence study.

Table 3.1 Abaqus Material Properties

Material	Elastic Modulus (ksi)	Poisson's Ratio	Assigned To
Steel	29,000	0.3	Mast Arm
Rigid	900,000,000	0.3	Loading Plate

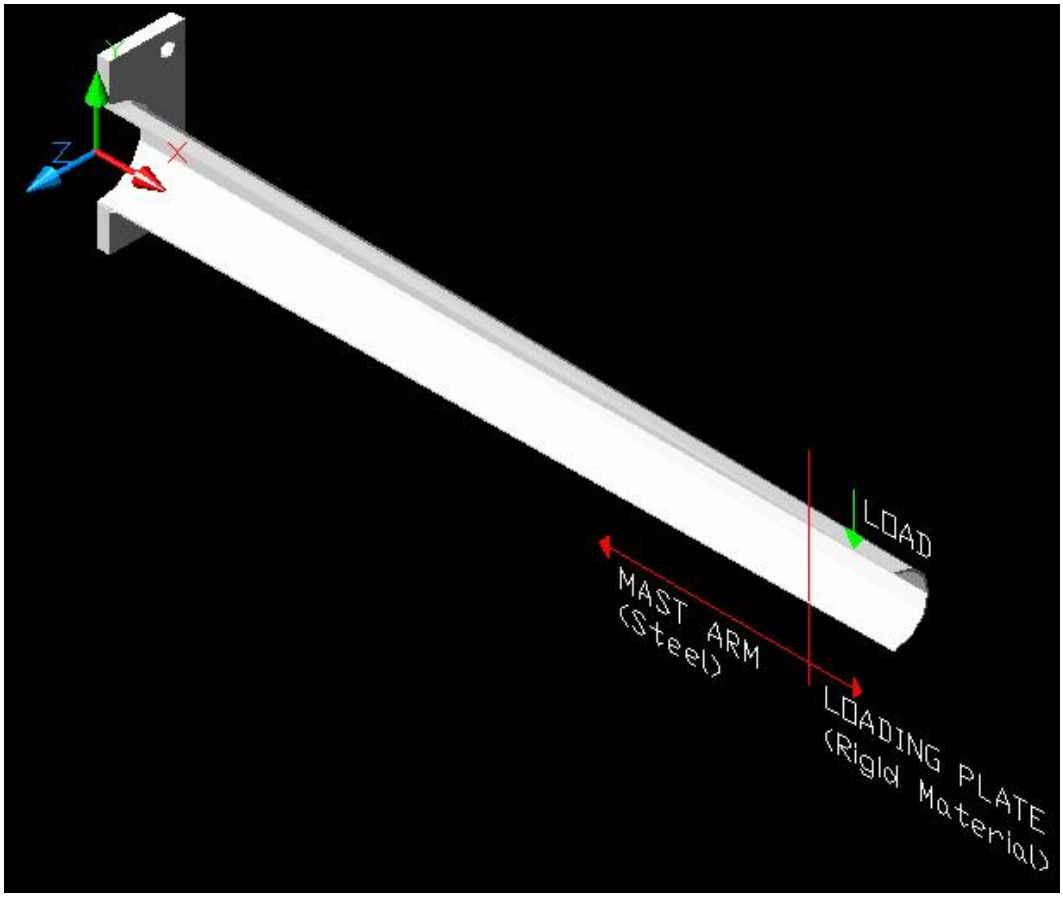

Figure 3.1 Solid Symmetric Model

Figure 3.2 shows a very fine mesh of element size 0.1 inches near weld toe. Figure 3.3 shows a slightly coarser mesh of element size 0.2 inches near weld toe.

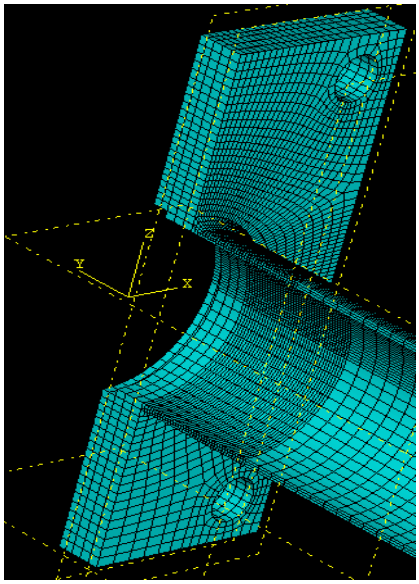

Figure 3.2 Fine Mesh

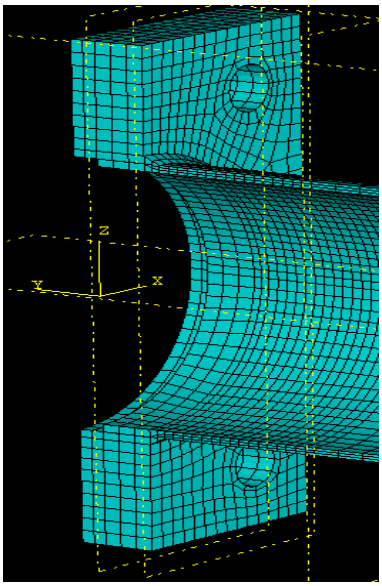

Figure 3.3 Coarse Mesh

3.3 STRESS CONCENTRATION FACTOR CALCULATION (SCF)

SCF is defined by Equation 3.1.

$$SCF = \frac{\text{Maximum Principal Stress at Weld Toe}}{\text{Maximum Bending Stress}} \qquad \text{Eq. 3.1}$$

To evaluate the maximum principal stress at weld toe, two approaches were taken as discussed in Section 3.3.1. The maximum bending stress (σ) is calculated using Equation 3.2

$$\sigma = Mc/I \qquad \text{Eq. 3.2}$$

where M and I are the Maximum Bending Moment and Moment of Inertia at the critical location respectively. c is the distance from the neutral axis to the top-most tension fiber of the mast arm at the critical location (i.e. at the weld toe).

Two different approaches were used in this study to determine the SCF. The first was to use the approach recommended by Det Norske Veritas (DNV). Second approach is to use Dong's Structural Stress approach [5].

3.3.1 DNV Technique

DNV report DNV-RP-C203 is the basis for this method. The nodal values of the principal stresses S_1 and S_2 at t/2 and 3t/2 respectively from the weld toe (t is the thickness of the mast arm) were extracted from Abaqus results and the stress at the weld found using Equation 3.3

.

$$S_o = (3S_1 - S_2)/2 \qquad \text{Eq. 3.3}$$

Figure 3.4 shows an example of stress extrapolation technique. Once S_o is obtained, it is substituted in the numerator of Equation 3.1 to determine the SCF. Sample calculation to determine SCF using DNV approach is described in Appendix A.

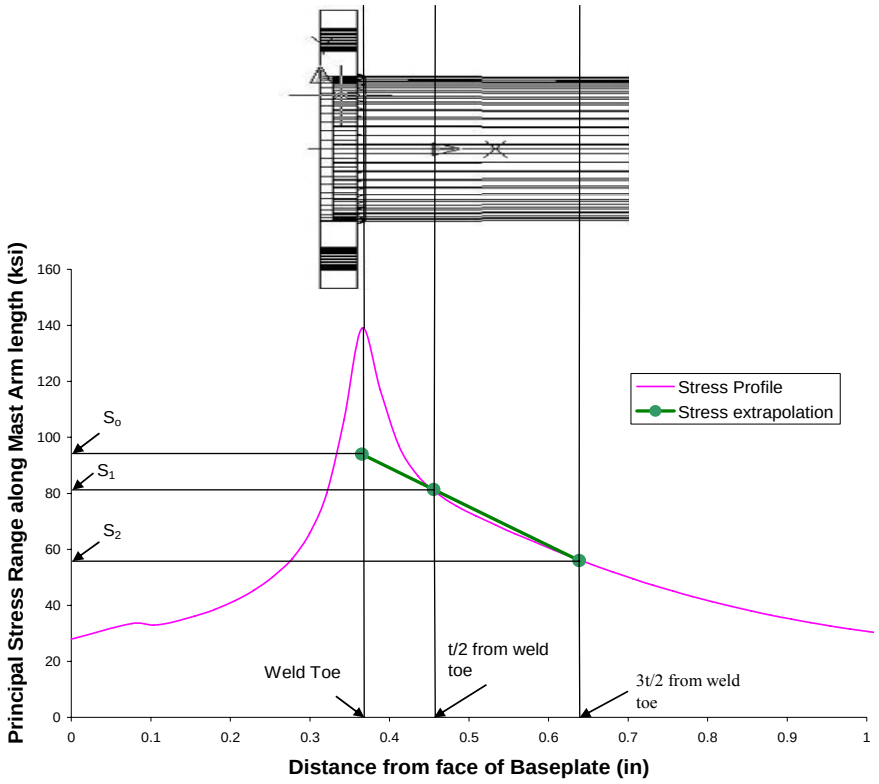

Figure 3.4 Stress Extrapolation

3.3.2 Structural Stress Technique

Dong [5] presented a mesh-size insensitive structural stress definition which is consistent with elementary structural mechanics theory. This approach provides a measure of a stress state that pertains to fatigue behavior of welded joints in the form of both membrane components (σ_m) and bending components (σ_b). According to Dong, the stress distribution at the T-fillet weld toe is assumed to exhibit a monotonic through-thickness distribution with the peak stress occurring at the weld toe as shown in Figure 3.5 (a). The corresponding statically equivalent structural stress distribution is illustrated in Figure 3.5 (b) in the form

of membrane component (σ_m) and bending component (σ_b) and is given by equation (3.4).

$$\sigma_s = \sigma_m + \sigma_b \qquad \text{Eq. 3.4}$$

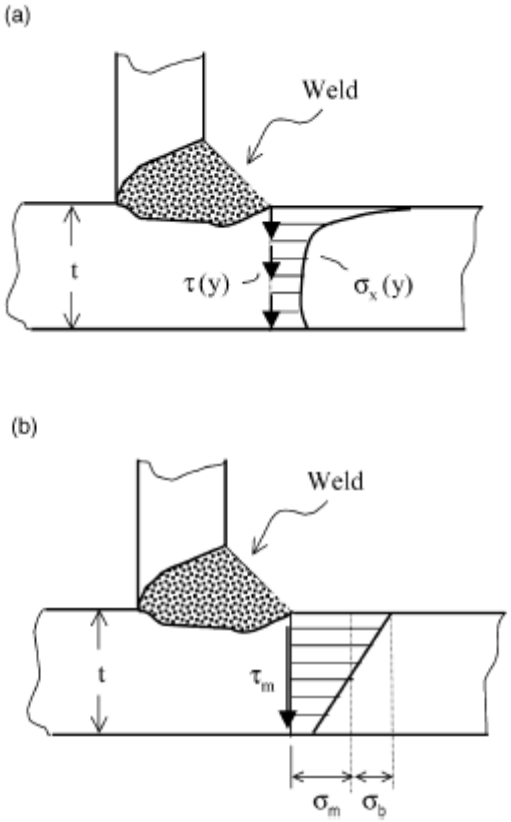

Figure 3.5 Structural stresses definition for through thickness fatigue crack. (a) Local through-thickness normal and shear stress at weld toe, (b) Structural stress definition at weld toe [5].

Dong defined the normal structural stress at a location of interest such as Section A-A at the weld toe in Figure 3.6 with a plate of thickness t. A second reference plane is defined along section B-B along which both normal and shear stresses can be directly obtained from a finite element solution. The distance, δ, represents the distance between sections A-A and B-B as shown in Figure 3.6. A

row of elements with same length of δ can be used in the finite element model for convenience. By imposing moment and axial equilibrium between sections A-A and B-B, the structural stress components σ_m and σ_b at section A-A must satisfy the equilibrium Equation 3.5 and Equation 3.6.

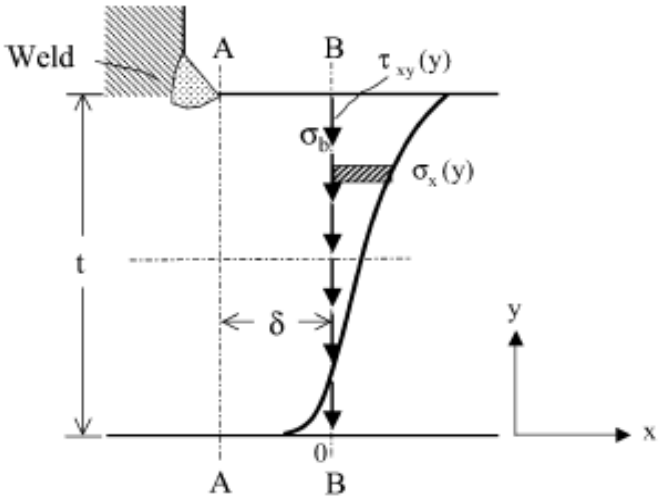

Figure 3.6 Structural stresses calculation procedure for through-thickness fatigue crack [5].

$$\sigma_m = 1/t * (\int_0^t \sigma_x(y).dy) \qquad \text{Eq. 3.5}$$

$$\sigma_m t^2/2 + \sigma_b t^2/6 = \int_0^t \sigma_x(y) \cdot y \cdot dy + \delta \cdot \int_0^t \tau_{xy}(y) \cdot dy \qquad \text{Eq. 3.6}$$

Since the transverse shear is negligible in all the analyses conducted, the integral representations of σ_m and σ_b in Equations 3.5 and 3.6 can be evaluated at section A-A of Figure 3.5. Using Equation 3.4, stress at the weld toe can be calculated and substituted in the numerator of Equation 3.1 to get the SCF. Sample calculations using Dong's Structural Stress approach is described in Appendix A.

3.4 CONVERGENCE STUDY

In order to arrive at mesh size to be used near weld toe, so as to get mesh-size insensitive results, convergence study was carried out using two geometries having different end plate geometry, arm thickness, and arm diameter. The geometries used for analysis are shown as Specimens 'A' and 'B' in Figure 3.7.

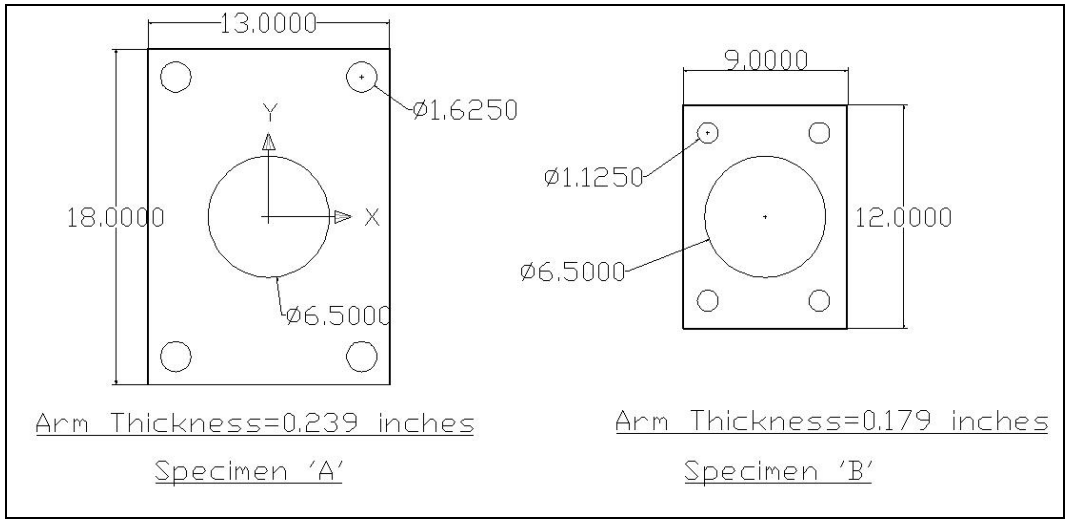

Figure 3.7 Two different geometries with end plate thickness of 1.5 inches used for convergence study

SCF values were calculated using both DNV and Dong's Structural Stress Approach. Tables 3.2 and 3.3 gives the SCF values obtained using Dong's Structural Stress approach for both specimens 'A' and 'B' respectively.

Table 3.2 Dong's Structural Stress Approach-Specimen 'A'

Mesh size near weld toe (in)	Membrane Component (σ_m)	Bending Component (σ_b)	Structural Stress (σ_s)	SCF	Difference in SCF between adjacent mesh size values (%)
0.1	28.779	61.603	90.382	4.734	0.637
0.15	28.805	61.011	89.816	4.704	0.814
0.2	28.568	60.523	89.091	4.666	0

Also, calculated were the differences in SCF values between adjacent mesh size values and as can been seen from Tables 3.2 and 3.3 the difference was less than 5% for both the specimens using DONG's Structural Stress approach. These results agree with DONG's mesh size insensitive approach.

Table 3.3 Dong's Structural Stress Approach-Specimen 'B'

Mesh size near weld toe (in)	Membrane Component (σ_m)	Bending Component (σ_b)	Structural Stress (σ_s)	SCF	Difference in SCF between adjacent mesh size values (%)
0.1	42.529	65.3	108	4.35	4.82
0.15	41.65	61.1	103	4.15	0.48
0.2	42.129	61.2	103	4.17	0

Figure 3.8 shows the plot, for Specimens ‘A’ and ‘B’, between SCF at weld toe obtained from DONG’s Structural Stress approach and different mesh sizes used for the study.

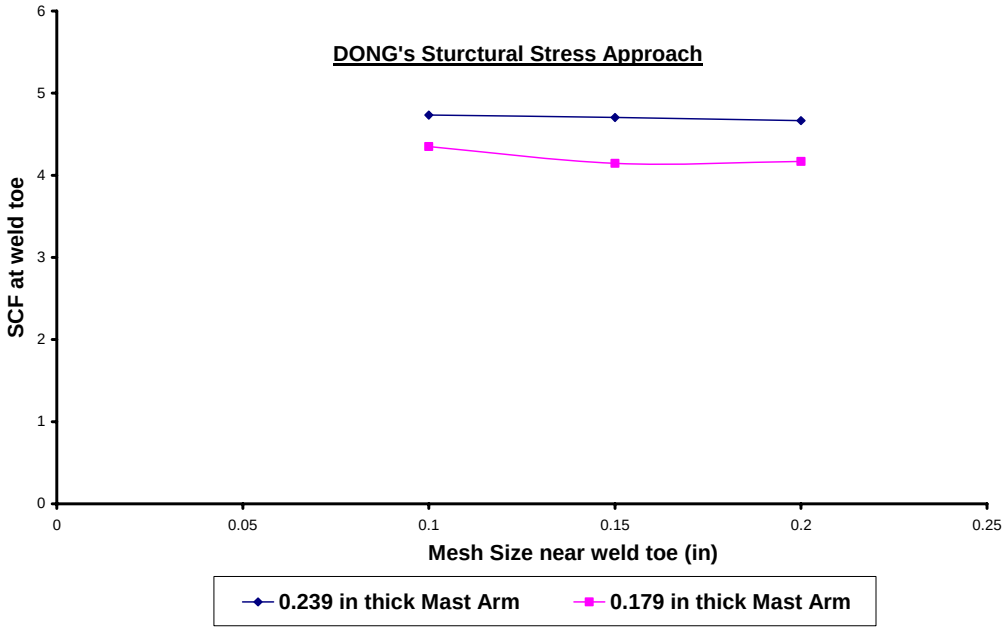

Figure 3.8 Mesh Convergence study using Dong’s Structural Approach

Using DNV approach, difference in SCF values were about 5% for specimen ‘A’ and somewhat higher for specimen ‘B’ as can be seen from Tables 3.4 and 3.5 respectively. With 6.5 inches mast arm outer diameter i.e. specimen ‘B’, mesh convergence is not good as per DNV approach. Figure 3.8 gives the plot between the SCF at weld toe obtained using DNV approach and mesh sizes for both the specimens.

Table 3.4 DNV Approach-Specimen 'A'

Mesh size near weld toe (in)	S_1 (Stress at t/2)	S_2 (Stress at 3t/2)	So = $(3S_1-S_2)/2$	SCF	Difference in SCF between adjacent mesh size values (%)
0.1	68.5	42	81.75	4.282	3
0.15	71	44.444	84.278	4.414	5.2
0.2	73.75	43.5	88.875	4.655	0

Table 3.5 DNV Approach-Specimen 'B'

Mesh size near weld toe (in)	S_1 (Stress at t/2)	S_2 (Stress at 3t/2)	So = $(3S_1-S_2)/2$	SCF	Difference in SCF between adjacent mesh size values (%)
0.1	91.5	66	104.25	4.205	7.74
0.15	97	65	113	4.558	2.2
0.2	98.5	64.5	115.5	4.659	0

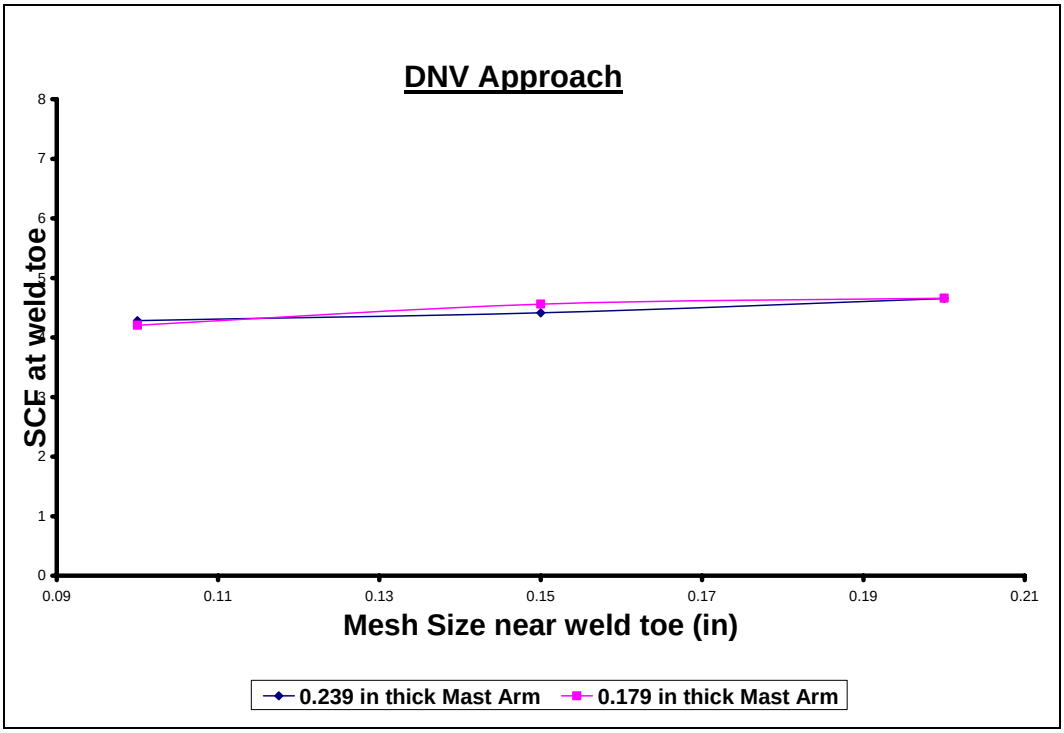

Figure 3.8 Mesh Convergence study using DNV Approach

Models with mesh size less than 0.1 inches could not be used because of greater memory capacity required to run those models. Also, greater convergence rate is obtained using Dong's Structural Stress approach for both specimens 'A' and 'B', compared to DNV approach. Since, for two specimens with different geometries, we get difference in SCF values less than 5% with Dong's approach, it was decided to use 0.1 inches for rest of the analysis.

CHAPTER 4
Analysis Results

4.1 INTRODUCTION

Finite element analyses done on the mast arm connections are presented and discussed in this chapter. Analyses are broadly classified into two components, first one concentrating on the effect of various geometric variables on SCF at weld toe and second concentrating on testing a hypothesis which states that fatigue life is some constant times the stress range (SCF x S_R) raised to the third power.

4.2 EFFECT OF GEOMETRIC VARIABLES ON SCF

Geometric variables evaluated to study their influence on the stress at the connection welds were:

- End plate thickness
- Mast arm Diameter
- Mast arm wall thickness
- Weld geometry

4.2.1 End plate thickness

Dong's Structural Stress and DNV approaches were used to study the effect of end plate thickness on SCF. The model geometry used for this study is shown in Figure 4.1 and consists of a tapered mast arm with 11 inches outer diameter and 0.239 inches thickness. Only variable in this study was end plate thickness. Analyses were conducted for six different end plate thicknesses such as 1 inch, 1.25 inches, 1.5 inches, 2 inches, 2.5 inches, and 3.0 inches.

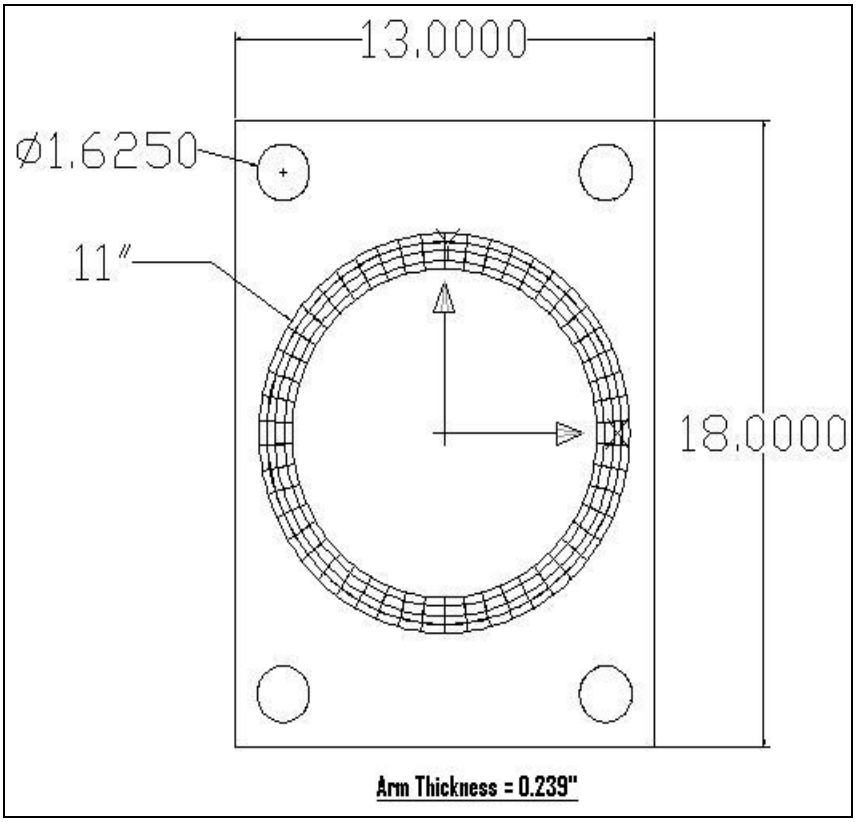

Figure 4. 1 Mast arm end plate geometry used for studying effect of end plate thickness on SCF

Abaqus analysis results used for determining the SCF at weld toe for estimating the effect of end plate thickness are given in appendices B and D.

Analysis results obtained using Dong's Structural approach and DNV approaches are compared in Figure 4.2.

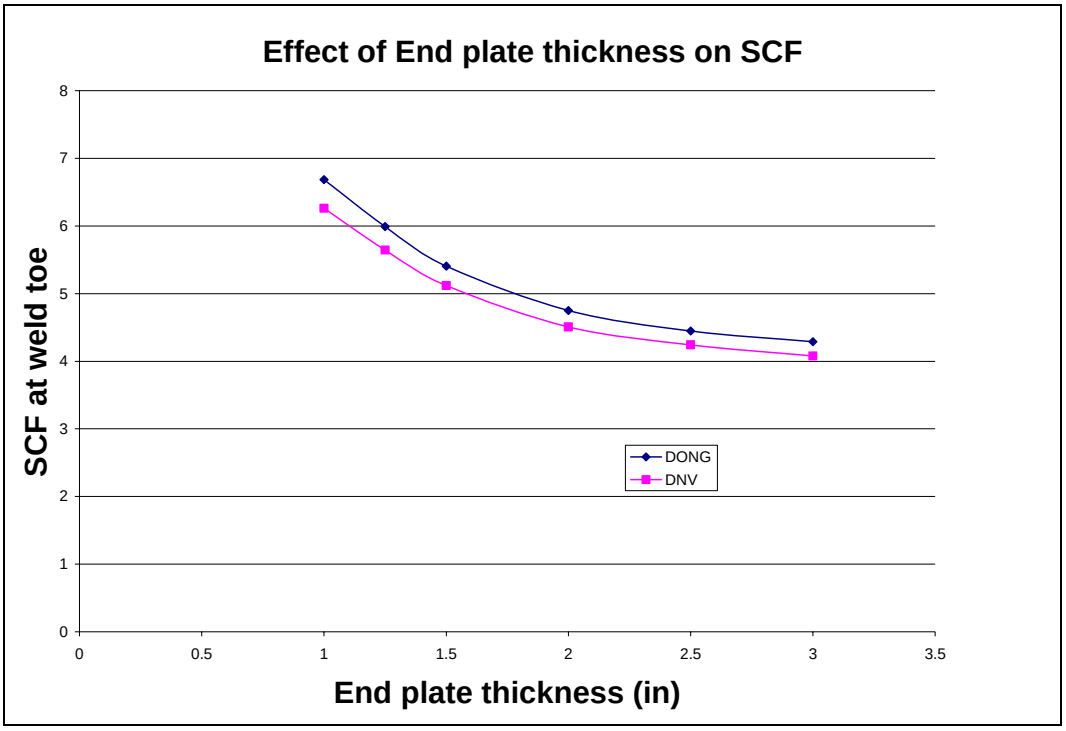

Figure 4. 2 Effect of end plate thickness-comparison of DNV and Dong's approaches

Figures 4.3 and 4.4 show that there is 20% reduction in SCF as the end plate thickness is increased from 1 to 1.5 inches and 35% reduction in SCF as the End plate thickness is increased from 1 to 3 inches. One can see that, SCF estimates using DONG's approach are higher than the one obtained using DNV approach. Both methods show a similar trend. The slope of SCF curve flattens as the end plate thickness is increased beyond 2 inches.

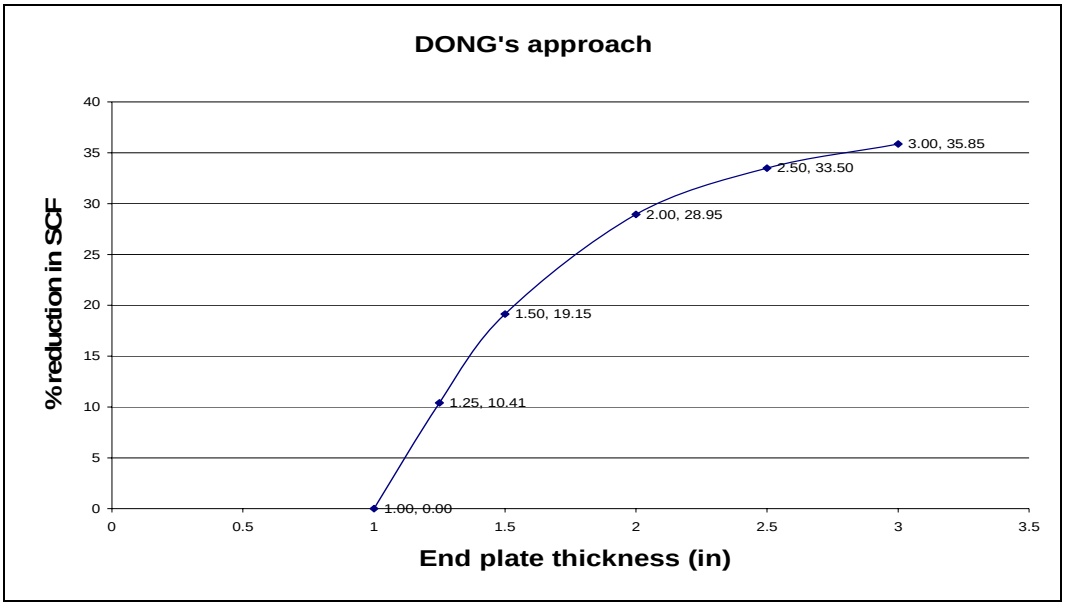

Figure 4. 3 Percent reduction in SCF relative to 1 in thick plate using Dong's approach

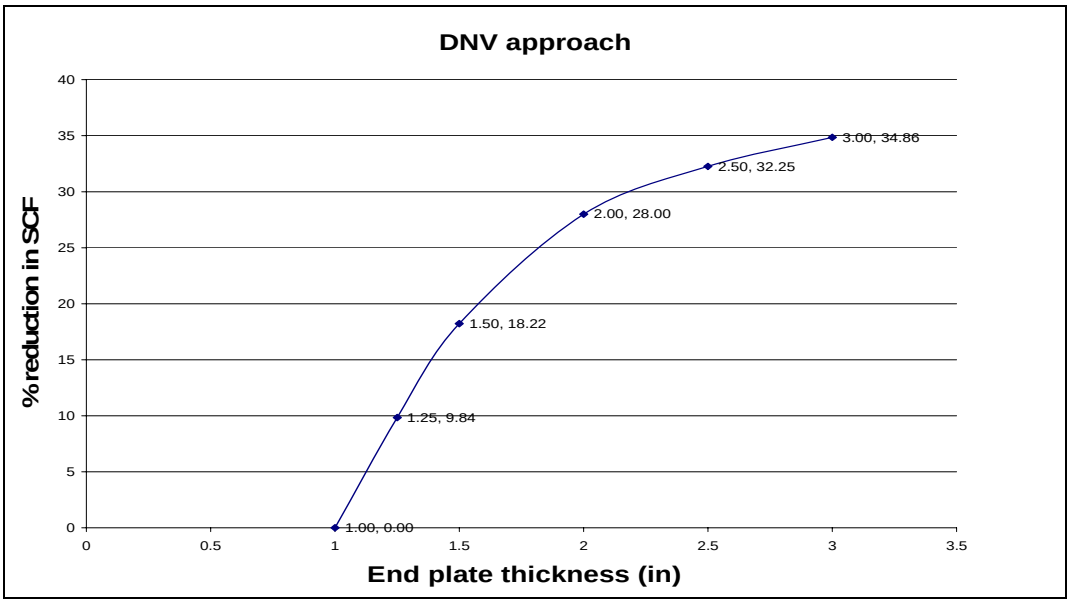

Figure 4. 4 Percent reduction in SCF relative to 1 in thick plate using DNV approach

4.2.2 Mast arm outer diameter

Front elevation and plan of the two models have the exact same end plate dimensions except for the Mast Arm base outer diameter and thickness as shown in Figures 4.5 and 4.6 respectively and were analyzed using DONG's Structural Stress and DNV approaches. Since it was found that end plate thickness has a major impact on SCF, the effect of Mast Arm base outer diameter was studied for different End plate thicknesses as shown in Figure 4.7.

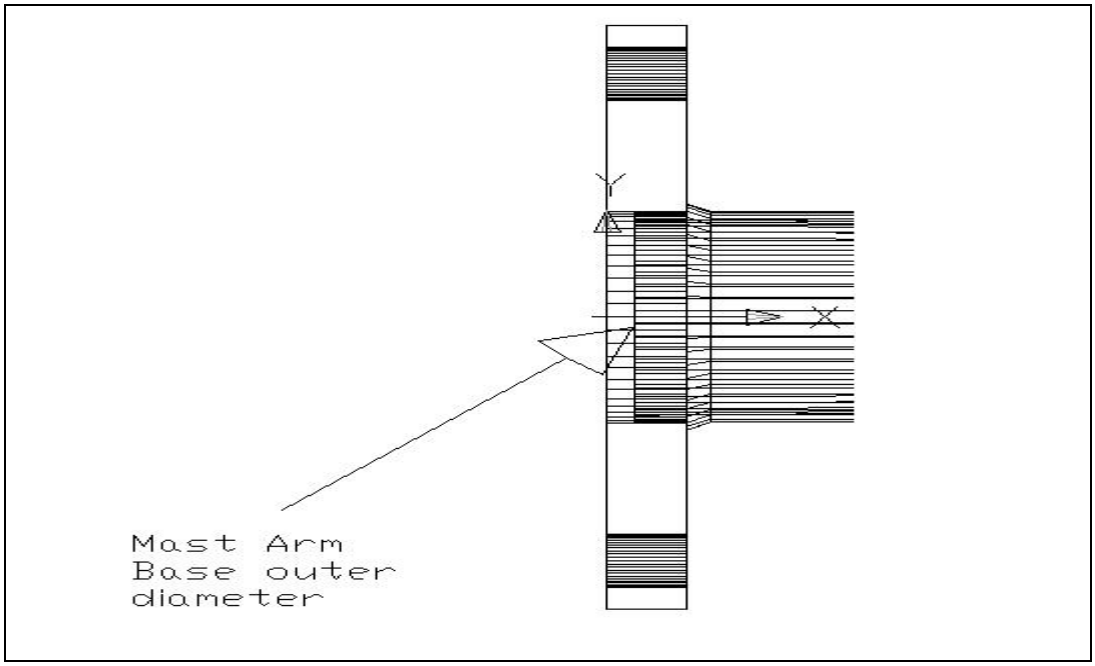

Figure 4. 5 Front Elevation showing Mast Arm base outer diameter

For this study mesh size used near weld toe was 0.239 inches and 0.179 inches for the 11 inch and 6.5 inch mast arm diameter respectively. It can be seen that the mesh size used near weld toe was same as the mast arm thickness.

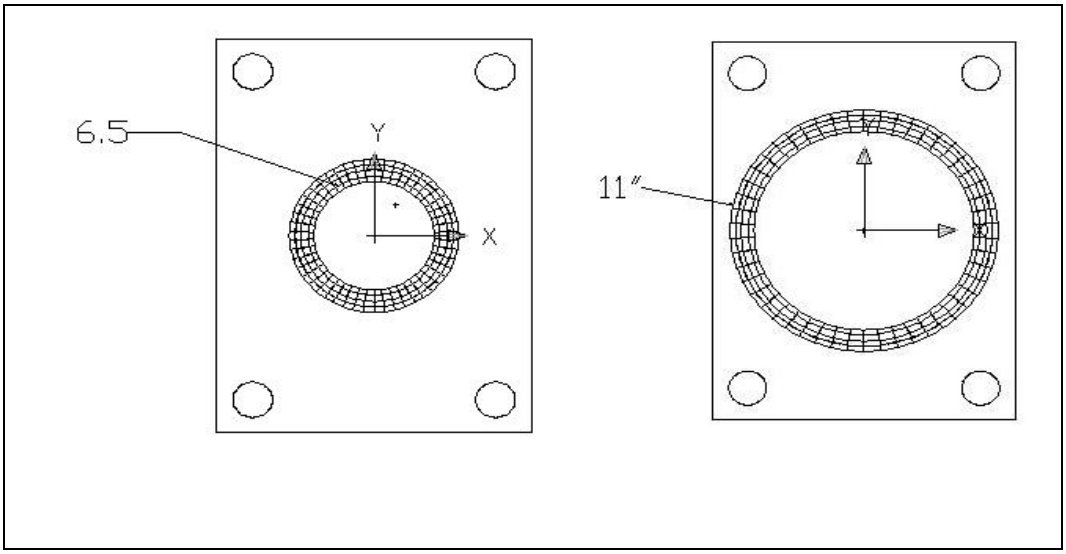

Figure 4. 6 6.5" and 11" Mast Arm base outer diameter

As can be seen from the Figure 4.7, SCF value is lower for 6.5 inches mast arm compared to the 11 inches mast arm for the same end plate thickness. It can also be seen that, 1 inch end plate on 6.5 inches mast arm produces approximately the same SCF value as 2 inches end plate on a mast arm of diameter 11 inches.

Also shown on the curve is the point corresponding to a full roller support condition. When the end plate thickness is increased, the slope of the curve flattens and stabilizes with the point corresponding to end plate with full roller support condition. This implies that the stiffness of the thicker end plate with their bottom half subjected to roller support boundary condition is almost equal to an end plate subjected to full roller support condition. Abaqus analysis results used for determining the SCF at weld toe to estimate the effect of mast arm outer diameter is given in appendices B and D.

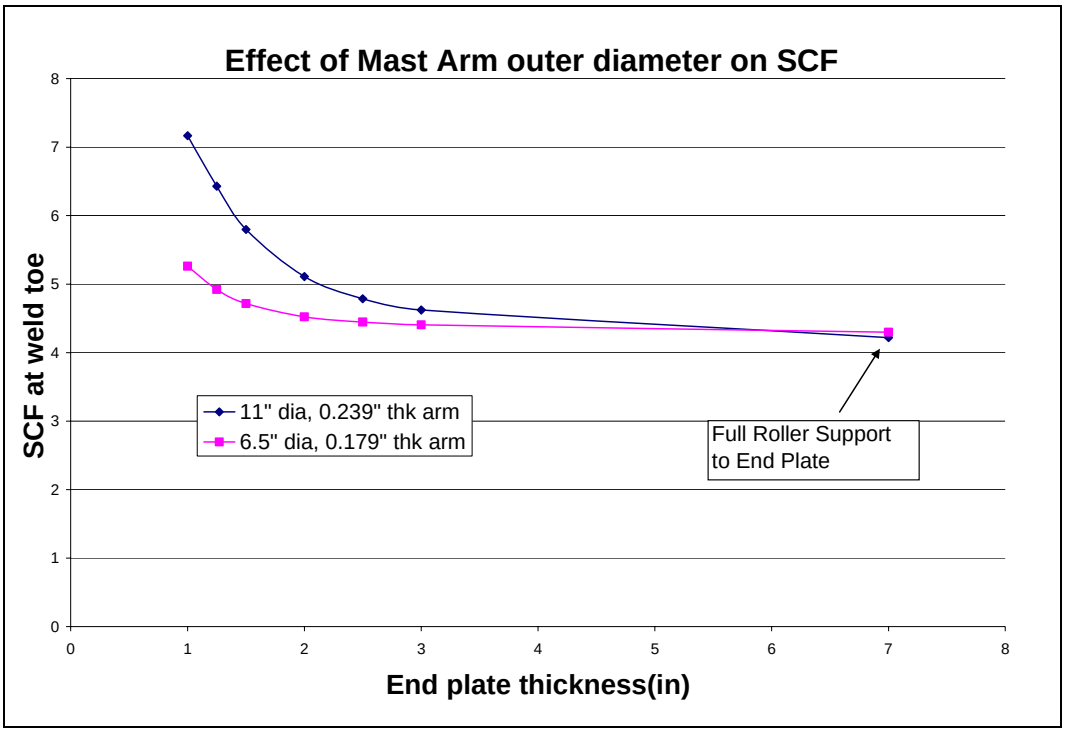

Figure 4. 7 Effect of Mast Arm Outer Diameter on SCF for different End plate thicknesses using DNV Approach

Another study was conducted on above geometries with the difference that, same mast arm thickness (0.239 inches) was used for both 6.5 inches and 11 inches mast arm outer diameter. Also, mesh size near weld toe was kept at 0.1 inches. The results are shown in Figures 4.8 and 4.9. For 11 inch diameter mast arm, SCF reduction with increase in end plate thickness followed a smooth pattern. However, for the 6.5 inch mast arm diameter, unexpected SCF reduction pattern at the weld toe was obtained near end plate thicknesses of 1 inch and 1.25 inches as shown in Figures 4.8 and 4.9 and hence need to be analyzed further.

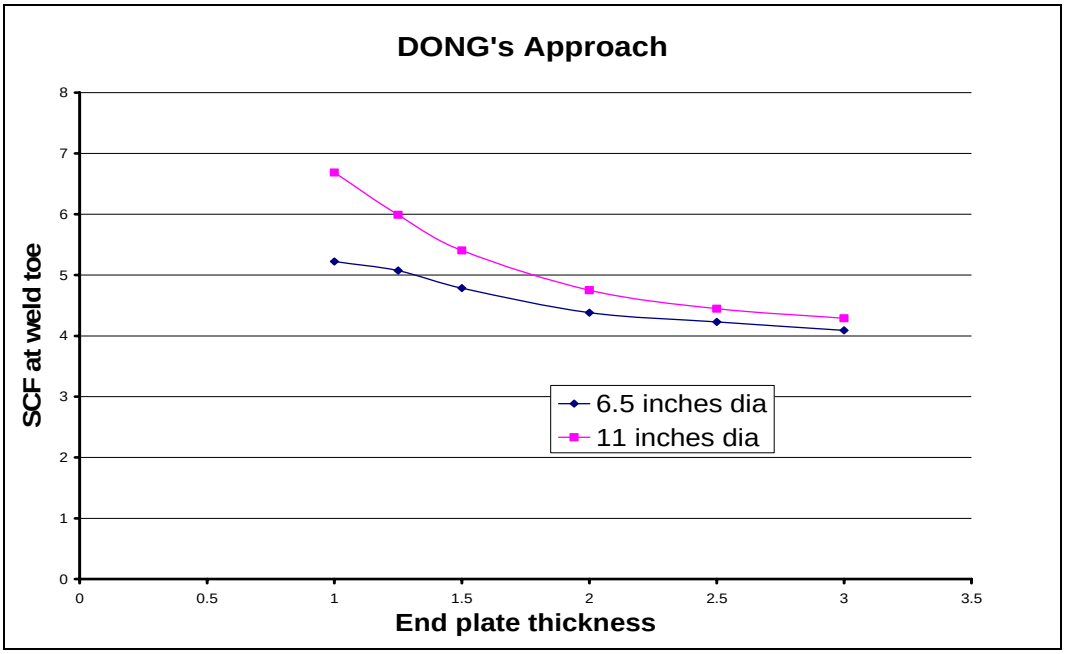

Figure 4. 8 Effect of Mast Arm Outer Diameter on SCF using DONG's Approach

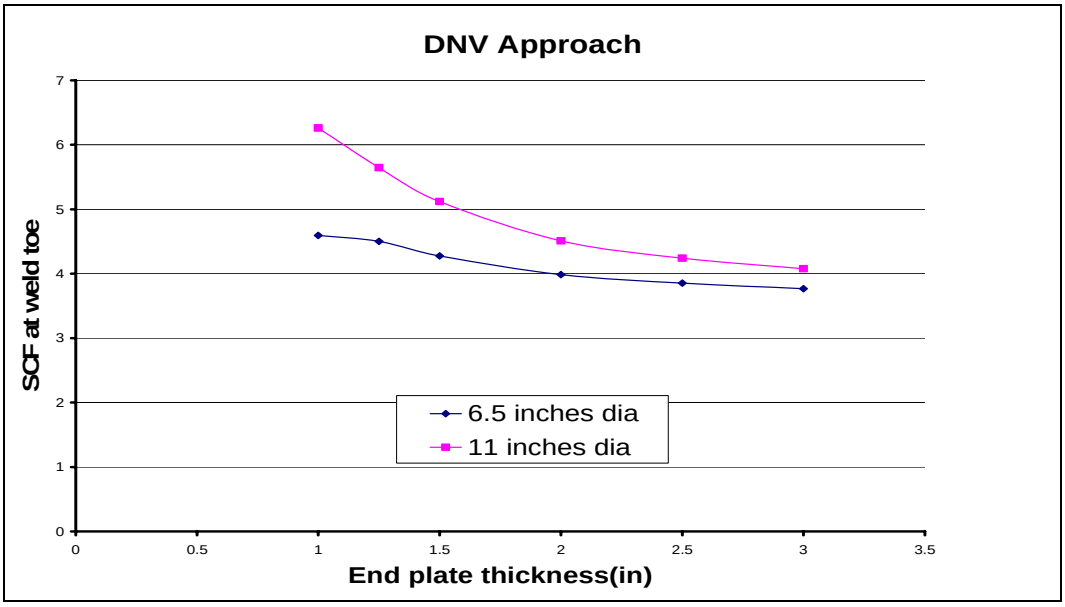

Figure 4. 9 Effect of Mast Arm Outer Diameter on SCF using DNV Approach

4.2.3 Weld Geometry

TXDOT specifications for arm base weld details are shown in Figure 4.10 for two different standard mast arm thickness. Effect of using weld details different from TXDOT specification, i.e., use of weld details corresponding to 3g pole for a 7g pole were studied using DNV approach and the results obtained are shown in Figure 4.11. TXDOT specifies use of 0.4375” x 0.25” for a 0.239” thick arm. In this study, two models were analyzed, one using weld details as per TXDOT specification and the other making use of smaller weld dimensions (0.3125” x 0.1875”) for a 0.239” thick arm. Different end plate thicknesses were used for this study. It can be seen from Figure 4.11 that having longer welds both on the Mast Arm and End plate decreases the SCF at weld toe and this reduction is significant for thinner plates. As we increase the end plate thickness, not much effect on stress at weld toe is caused by weld details.

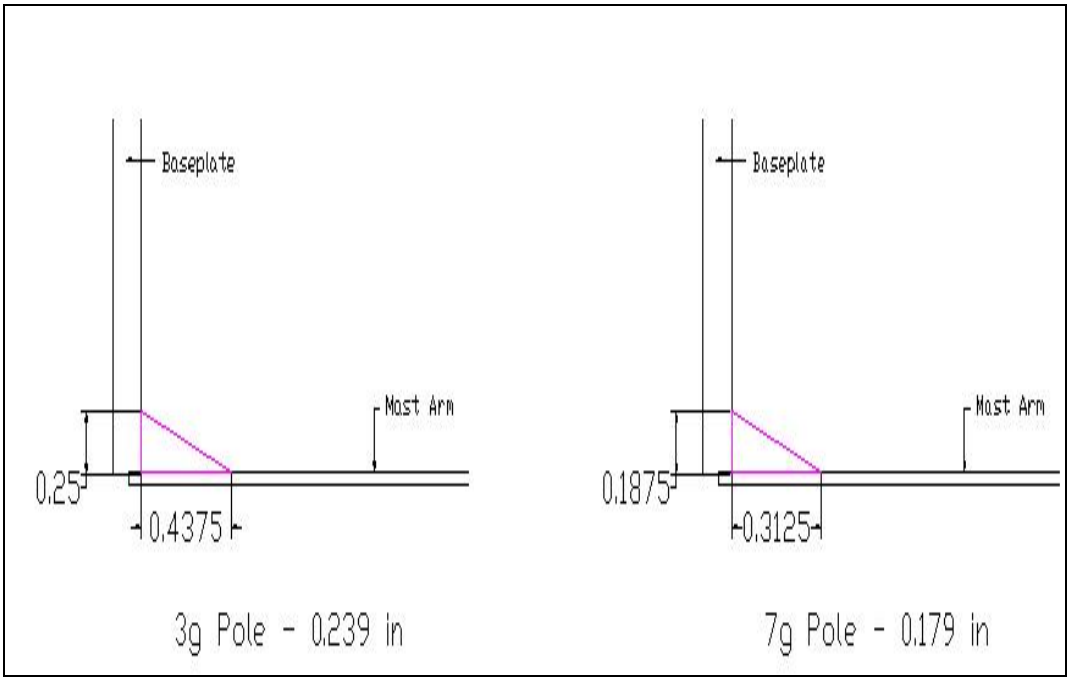

Figure 4. 10 TXDOT specifications for Arm Base Weld details

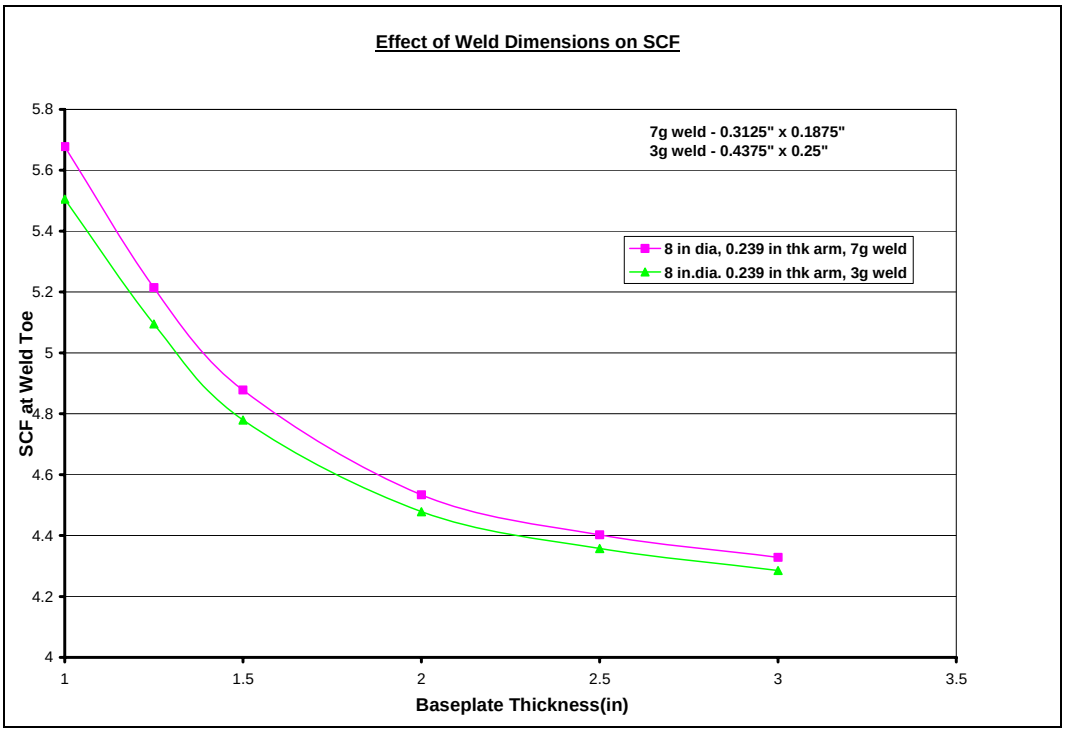

Figure 4. 11 Effect of Weld Geometry for different End plate thicknesses using DNV Approach

Also studied was the effect of equal and unequal weld on stresses at weld toe. It is evident from Figure 4.12 that using unequal weld with longer leg (LL) on mast arm and shorter leg (SL) on end plate leads to least stress values at weld toe. This improvement related to unequal leg fillet weld was attributed to the contact angle of the weld which is lesser than an equal leg fillet weld. Abaqus analysis results used for determining the effect of weld dimensions and weld orientation on stresses at weld toe are given in appendices B and C respectively.

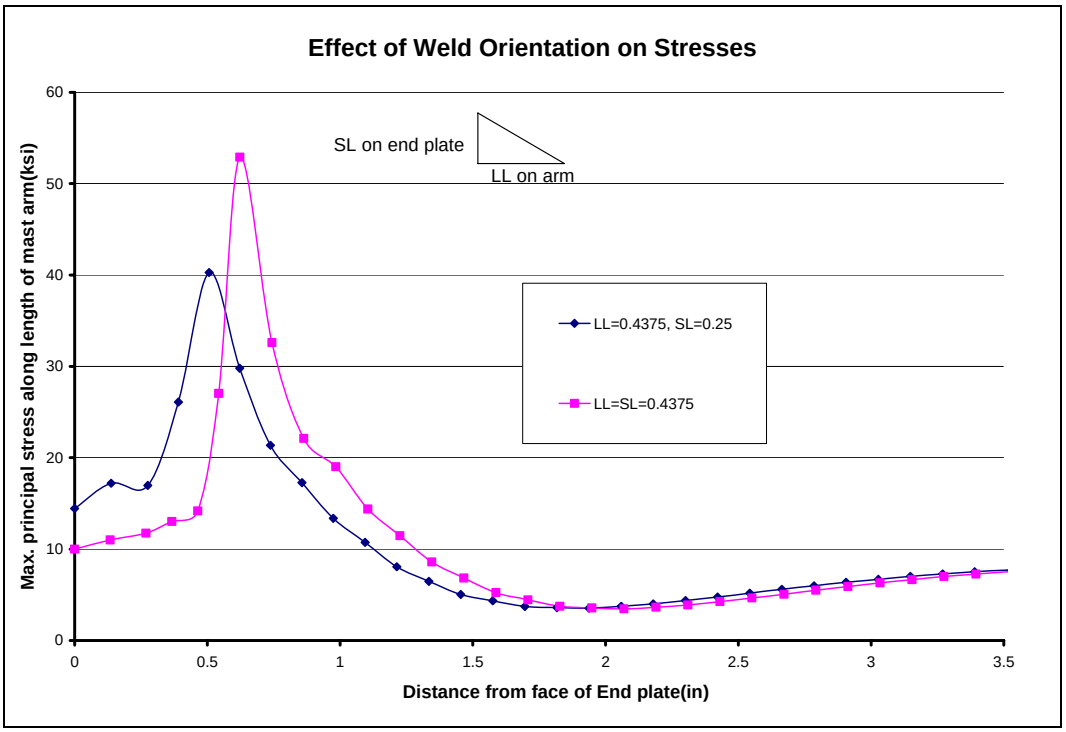

Figure 4. 12 Effect of Weld Orientation on Maximum Principal Stress along Mast Arm Length

4.2 HYPOTHESIS INVESTIGATION

The hypothesis relating fatigue life to stress range is

$$N = A \cdot S_R^3 \qquad \text{Eq. 4.1}$$

where N is the fatigue life, A = Fatigue Life Coefficient, S_R is the maximum stress range at weld toe. Specimens belonging to Valmont Industry, Nippon Steel, and TXDOT were tested at Ferguson Structural Engineering Laboratory, The University of Texas at Austin as part of various research projects. SCF of these specimens were obtained from finite element study using Abaqus. Various analyzed models along with their geometries are given in the Table 4.1.

Table 4. 1 Analyzed Models

Model	End plate thickness (in.)	End plate Height (in.)	End plate Width (in.)	Bolt Hole Diameter (in.)	Bolt Hole Offset from Corner (in.)	Mast Arm Wall Thickness(in.)	Mast Arm base outer φ (in.)
TXu	1.5	19	19	1.5625	2	0.239	10
VALu	1.5	19	19	1.5625	2	0.179	10
VALNu	1.5	19	19	1.5625	2	0.179	10
VALNu2	2	19	19	1.5625	2	0.179	10
Nippon steel							
A	1.5	19	12	1.5625	2	0.1793	10
B	1.75	20	20	1.8125	3.3	0.239	13

Using the nominal stress range values under which the specimens are tested in the laboratory and SCF obtained from finite element study, maximum stress range at weld toe is obtained using Equation 2.1. SCF values obtained from the finite element analysis using both DONG's and DNV approaches are shown in Tables 4.2 and 4.3 respectively. These stress ranges are plotted against fatigue life of the specimens which are obtained from experiments as shown in Figures 4.11 and 4.12. Regression analysis is used to determine the best fit straight line for the data obtained using both approaches and the results shown in Table 4.5. Abaqus analysis results used for determining the SCF values for hypothesis investigation study are given in Appendices B and D.

Table 4. 2 Stress Concentration Factor using DONG's Approach

Model	Maximum Bending Stress range (σ)	Membrane component (σ_m)	Bending component (σ_b)	Structural Stress (σ_s)	SCF
TXu	5.89	7.38	26.31	33.69	5.72
VALu	7.72	10.98	34.71	45.69	5.92
VALNu	7.72	12.65	26.88	39.52	5.12
VALNu2	7.72	10.98	34.72	45.71	5.92
Nippon steel					
A	7.69	12.87	28.55	41.42	5.39
B	3.42	4.26	11.81	16.07	4.70

Table 4. 3 Stress Concentration Factor using DNV Approach

Model	Maximum Bending Stress range (σ)	Stress at t/2 from weld toe (S1)	Stress at 3t/2 from weld toe (S2)	Stress at weld toe (So)	SCF
TXu	5.89	26.5	17	31.25	5.31
VALu	7.72	38.5	26.25	44.63	5.78
VALNu	7.72	34	24.5	38.75	5.02
VALNu2	7.72	38.25	26.25	44.25	5.73

Nippon steel					
A	7.69	36	26	41	5.33
B	3.42	13.25	9.25	15.25	4.46

Table 4. 4 S-N values obtained using two approaches

Model	**Nominal Stress range at socket weld**	**Fatigue Life (N)**	**Stress range at weld toe (DONG)**	**Stress range at weld toe (DNV)**
VALuA	11.9	249446	70.42	68.78
VALuB	11.9	453948	70.42	68.78
VALuC	6.3	2072592	37.28	36.41
TXuA	6	2199343	34.33	31.85
TXuB	6.1	2816706	34.91	32.38
TXuC	11.8	177596	67.52	62.64
TXuD	12	194694	68.67	63.70
VALNu A	11.9	389428	70.45	68.20
VALNu B	11.8	265540	69.86	67.63
VALNu 2A	11.9	5144528	60.91	59.72
VALNu 2B	11.8	1683127	60.40	59.22
Nippon steel				
A1	12.5	195752	67.33	66.65
A2	12.6	126325	67.87	67.18
B1	12.7	79690	59.74	56.69
B2	12.7	79691	59.74	56.69

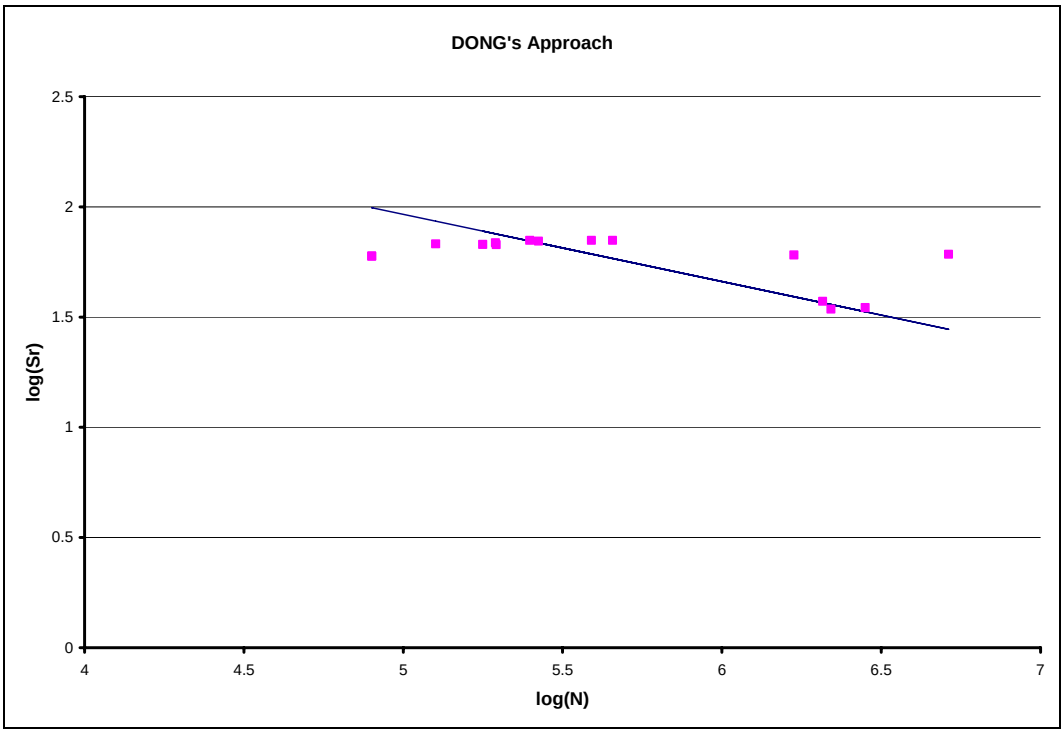

Figure 4. 13 Hypothesis investigation using DONG's Approach

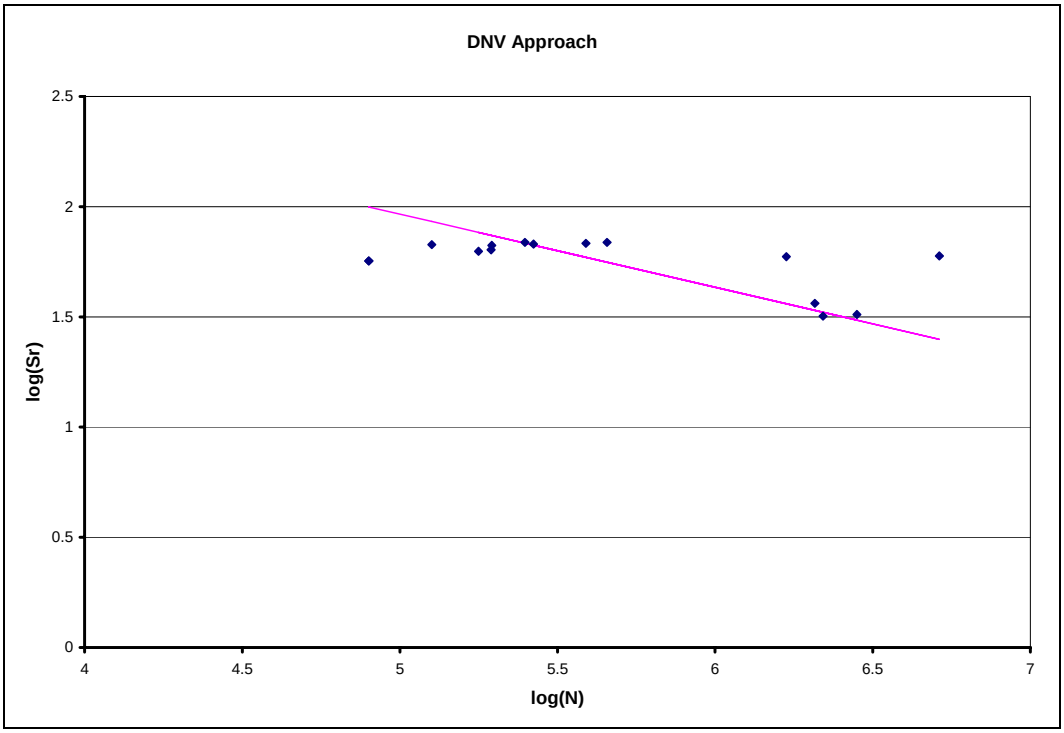

Figure 4. 14 Hypothesis investigation using DNV Approach

Table 4. 5 Hypothesis Investigation Results

DNV	$N = A \cdot S_R^{3.0156}$	**A = 10.9282**
DONG	$N = A \cdot S_R^{3.2804}$	**A = 11.448**

When Nominal Stress range was plotted against Fatigue Life, there was found larger scatter in the experimental data. This scatter was reduced by plotting SCF x Nominal Stress range versus Fatigue Life. Some of the experimental values had very large Fatigue Life and were marked as “run out”. Those data were not used for the above hypothesis investigation.

CHAPTER 5
Conclusions and Recommended Research

5.1 CONCLUSIONS

- End plate thickness, one of the causes for end plate flexibility, was found to have major effect on SCF at weld toe compared to other geometric variables analyzed.
    1. For a mast arm with 11 inches outer diameter, increase of end plate thickness from 1 inch to 1.5 inches gave a 20% reduction in SCF and only 4% reduction in SCF when the end plate thickness was increased from 2.5 inches to 3 inches. This can be attributed to the fact that stiffness of the end plate is directly proportional to the end plate thickness raised to the power three. For end plate thickness increase from 1 to 1.5 inches, stiffness of the end plate is increased by 3.4 times and for the increase in end plate thickness from 2.5 to 3 inches, stiffness is increased by 1.7 times. This explains the result obtained above.
    2. However, less reduction in SCF with increase in end plate thickness was observed for a 6.5 inches mast arm outer diameter. The SCF was reduced by around 8% as the end plate thickness was increased from 1 inch to 1.5 inches and around 2% for increase in end plate thickness from 2.5 inches to 3 inches.

- As the mast arm outer diameter is decreased, SCF at weld toe was found to decrease for a given end plate geometry.
    1. For an end plate thickness of 1 inch, change in mast arm diameter from 11 inches to 6.5 inches reduced the SCF at weld toe by 36%. This is because hole in the end plate is the same as the mast arm outer diameter as the mast arm is socketed into the end plate. Hence greater loss of material for an end plate with a hole of 11 inches than those with 6.5 inch hole, keeping all other variables constant, and as a result stiffness or rotational restraint is lesser for the former. Also, moment induced in end plate is larger for a larger diameter mast arm than a smaller diameter mast arm, for the same stresses.
    2. With higher end plate thicknesses, reduction in SCF at weld toe, with decrease in mast arm outer diameter, is comparatively lesser. For example, as the mast arm outer diameter is changed from 11 inches to 6.5 inches, reduction in SCF at weld toe is around 20% for an end plate thickness of 1.5 inches and around 8% for an end plate thickness of 3 inches. Again lesser flexibility of thicker end plate might be the cause for the above observation.
- As mast arm thickness is increased from 0.179 inches to 0.239 inches, SCF at weld toe decreases and again this reduction is significant for thinner plates from 1 to 1.5 inches.
- Effect of weld dimensions (long leg and short leg dimensions of the weld) on SCF at weld toe tends to decrease with increase in end plate thickness. Unequal weld with longer leg on mast arm and shorter leg on end plate

reduces the stress at the weld toe to a greater extent compared to equal welds and the geometry which has longer leg on end plate and shorter leg on mast arm.

- Results obtained using Dong's Structural Stress approach is higher than those obtained using DNV approach. Also it is observed that with decrease in mesh size, SCF at weld toe increases for Dong's Structural Stress approach whereas decreases for DNV approach. The cause may be attributed to the difference in the stress evaluation technique of the two approaches.
- From the hypothesis investigation, we can conclude that scatter in the experimental data is reduced when maximum stress range at weld toe (SCF x Nominal stress range) plotted against Fatigue life as compared to the plot between Nominal stress range and Fatigue life.

5.2 RECOMMENDATIONS FOR FUTURE RESEARCH

This study analyzed the effect of few geometric variables on SCF at weld toe. One of the factors affecting end plate flexibility, namely the end plate thickness, was studied. But other factors like bolt spacing, end plate dimensions like square or rectangular geometry, and end plate side length (distance between the outer edge of the arm and the edge of the end plate) need to be analyzed and their effect on SCF need to be quantified. By doing this we can have a clear picture of the effect of various factors contributing to end plate flexibility on SCF at weld toe. The plot of SCF versus end plate thickness for 6.5 inches mast arm was not smooth and hence this geometry needs to be analyzed further.

APPENDIX A

Calculation of Nominal Bending Stress range (σ) to be used for both DNV and Dong's Structural Stress Approach

$\sigma = Mc / I$

M = Maximum moment at the critical section

I = Moment of Inertia at the critical section

$$I = \frac{\pi(d_0^4 - d_i^4)}{64}$$

c = Distance of the top most tension fiber of an unstiffened mast arm from the neutral axis

$c = d_0 / 2$

d_o = Outer diameter at weld toe

d_i = Inner diameter at weld toe

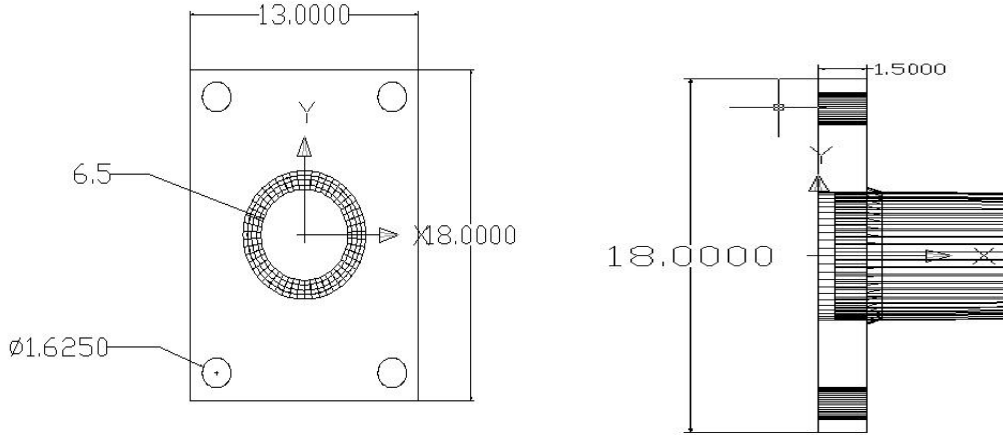

Appendix A- 1 Mast Arm – End plate geometry used

Mast Arm is 90" in length and tapers with a slope of 1 in 0.006. Load applied is 1.5 kips. For the geometry shown above and using the above formulae we get,

M = 135 kip-in

d_o = 6.488in, d_i = 6.01in, c = 3.244in, I = 22.93634 in^4

σ = 19.09372 ksi

Table A- 1 DNV Approach

Mesh size near weld toe	S_1(stress at t/2)	S_2(stress at 3t/2)	$S_0=(3S_1-S_2)/2$	SCF
0.1	68.5	42.000	81.750	4.282
0.15	71	44.444	84.278	4.414
0.2	73.75	43.500	88.875	4.655

SCF for 0.1" mesh size = 81.75/19.09372 = 4.282

Table A- 2 Dong's Structural Stress Approach

Mesh size near weld toe	Membrane comp (σ_m)	Bending Comp (σ_b)	Structural Stress (σ_s)	SCF
0.1	28.779	61.603	90.382	4.734
0.15	28.805	61.011	89.816	4.704
0.2	28.568	60.523	89.091	4.666

SCF for 0.1" mesh size = 90.3817/19.09372 = 4.734

APPENDIX B

Results obtained from the Abaqus analysis to be used for calculating SCF using DNV technique are given in this section. The following tables give the distance of points from the face of end plate along the length of mast arm and maximum principal stress values corresponding to those points. From these values, a graph is drawn and values S_1 and S_2 which are respectively at distances t/2 and 3t/2 from weld toe are obtained. These values are then used to determine the stress at weld toe (S_o) using Equation 3.3. So is then substituted in the numerator of Equation 3.1 to determine the SCF at weld toe. The highlighted value in the table corresponds to the stress where weld toe is located.

Table B- 1 Abaqus analysis results for Mesh Convergence study using DNV approach- Specimen 'A'

0.1 inch		0.15 inch		0.2 inch	
Distance from face of end plate (in)	Max. Principal stress (ksi)	Distance from face of end plate (in)	Max. Principal stress (ksi)	Distance from face of end plate (in)	Max. Principal stress (ksi)
0	17.0321	0	16.4757	0	16.3983
6.74E-02	24.2477	1.00E-01	27.5532	1.01E-01	27.462
1.35E-01	31.1237	2.01E-01	36.8183	2.01E-01	37.4665
1.84E-01	38.5825	2.83E-01	71.0303	2.83E-01	71.9343
2.33E-01	44.9775	**3.65E-01**	**129.392**	**3.65E-01**	**126.107**
2.71E-01	56.1432	4.41E-01	102.063	4.65E-01	95.4859
3.09E-01	75.453	5.17E-01	77.2856	5.65E-01	71.1714
3.37E-01	111.932	5.93E-01	69.7405	6.64E-01	62.1521
3.65E-01	**146.733**	6.69E-01	60.9832	7.64E-01	52.0216
4.15E-01	111.173	7.45E-01	54.8182	8.64E-01	46.2937
4.65E-01	87.7422	8.21E-01	48.2396	9.63E-01	40.5716
5.15E-01	78.9212	8.97E-01	44.0857	1.06276	37.7623
5.65E-01	73.1169	9.73E-01	40.2449	1.16238	35.4199
6.15E-01	68.107	1.04851	38.1225	1.262	34.8404

Table B- 2 Abaqus analysis results for Mesh Convergence study using DNV approach- Specimen 'B'

0.1 inch		0.15 inch		0.2 inch	
Distance from face of end plate (in)	Max. Principal stress (ksi)	Distance from face of end plate (in)	Max. Principal stress (ksi)	Distance from face of end plate (in)	Max. Principal stress (ksi)
0	37.7303	0	20.1624	0	37.1155
9.02E-02	44.413	1.04E-01	29.9318	1.04E-01	43.9161
1.80E-01	40.475	2.09E-01	31.5916	2.09E-01	40.3797
2.47E-01	42.1543	2.90E-01	32.1809	2.90E-01	44.2145
3.14E-01	46.2894	3.71E-01	39.0834	3.70E-01	53.9682
3.67E-01	54.0885	4.38E-01	66.947	4.38E-01	82.0371
4.20E-01	67.0223	**5.05E-01**	**109.359**	**5.05E-01**	**113.855**
4.63E-01	93.6172	5.75E-01	87.8367	6.00E-01	80.7201
5.05E-01	**123.268**	6.46E-01	65.8305	6.95E-01	58.7192
5.50E-01	98.9197	7.18E-01	56.7025	7.92E-01	49.92
5.96E-01	76.314	7.90E-01	49.7469	8.90E-01	41.2009
6.43E-01	65.1037	8.64E-01	44.4439	9.88E-01	35.5331
6.91E-01	59.9178	9.37E-01	38.1009	1.08628	29.5611
7.39E-01	55.9928	1.01116	33.7605	1.18524	26.2147
7.88E-01	50.5924	1.08517	29.6582	1.2842	23.1933
8.37E-01	46.2279	1.1595	27.0664	1.38347	21.9163

Table B- 3 Abaqus analysis results for TXu specimen

Distance from face of end plate (in)	Max. Principal Stress (ksi)
0	14.8066
7.64E-02	18.5645
1.53E-01	16.5148
2.08E-01	16.2551
2.64E-01	17.2596
3.11E-01	19.0954
3.58E-01	20.4367
3.99E-01	23.1778
4.40E-01	28.8765
4.73E-01	38.8814
5.06E-01	47.7952
5.51E-01	37.6396
5.96E-01	29.4911
6.43E-01	25.3714
6.90E-01	23.4748
7.38E-01	21.9472
7.87E-01	19.8759
8.36E-01	18.0892
8.84E-01	16.3198
9.34E-01	14.8097
9.83E-01	13.2877
1.03284	12.0259

Table B- 4 Abaqus analysis results for VALu specimen

Distance from face of end plate (in)	Max. Principal Stress (ksi)
0	15.354
6.72E-02	19.1628
1.34E-01	19.0922
1.83E-01	21.04
2.33E-01	22.8763
2.71E-01	26.8794
3.09E-01	34.5636
3.38E-01	49.1914
3.66E-01	62.7444
4.16E-01	46.9168
4.66E-01	36.6901
5.16E-01	32.6753
5.66E-01	29.9068
6.16E-01	27.374
6.66E-01	24.3037
7.16E-01	21.7919
7.65E-01	19.3754
8.15E-01	17.413
8.65E-01	15.4267
9.15E-01	13.8594
9.65E-01	12.2964
1.01494	11.0948
1.06483	9.89688

Table B- 5 Abaqus analysis results for VALNu specimen

Distance from face of end plate (in)	Max.Principal Stress (ksi)
0	15.3609
6.72E-02	19.1713
1.34E-01	19.1005
1.83E-01	21.0492
2.33E-01	22.8859
2.71E-01	26.8911
3.09E-01	34.5787
3.38E-01	49.2124
3.66E-01	62.7715
4.16E-01	46.937
4.66E-01	36.7059
5.16E-01	32.6894
5.66E-01	29.9197
6.16E-01	27.3857
6.66E-01	24.3141
7.16E-01	21.8012
7.65E-01	19.3837
8.15E-01	17.4205
8.65E-01	15.4333
9.15E-01	13.8654
9.65E-01	12.3017
1.01494	11.0995
1.06483	9.90111

Table B- 6 Abaqus analysis results for VALNu2 specimen

Distance from face of end plate (in)	Max. Principal stress (ksi)
0	9.2953
7.72E-02	11.8495
1.54E-01	13.7751
2.13E-01	16.9524
2.72E-01	21.3714
3.19E-01	34.062
3.66E-01	**52.3893**
4.16E-01	41.8371
4.66E-01	32.6897
5.16E-01	29.5855
5.66E-01	27.4913
6.16E-01	25.5556
6.66E-01	23.1248
7.16E-01	21.142
7.65E-01	19.2477
8.15E-01	17.7109
8.65E-01	16.1516
9.15E-01	14.9237
9.65E-01	13.6986
1.01494	12.7586
1.06483	11.8207

Table B- 7 Abaqus analysis results for Nippon Steel A specimen

Distance from face of end plate (in)	Max. Principal Stress (ksi)
0	9.0639
6.74E-02	11.8497
1.35E-01	14.0468
1.84E-01	16.7187
2.33E-01	18.7667
2.71E-01	22.7533
3.09E-01	30.1081
3.37E-01	44.0091
3.65E-01	57.1621
4.15E-01	43.4902
4.65E-01	34.6297
5.15E-01	31.2757
5.65E-01	29.0868
6.15E-01	27.0581
6.65E-01	24.5408
7.15E-01	22.4767
7.65E-01	20.4981
8.14E-01	18.8854
8.64E-01	17.2498
9.14E-01	15.9544
9.64E-01	14.6613
1.0139	13.6625

Table B- 8 Abaqus analysis results for Nippon Steel B specimen

Distance from face of end plate (in)	Max. Principal Stress (ksi)
0	5.24913
7.65E-02	6.2987
1.53E-01	6.27617
2.08E-01	6.61475
2.64E-01	7.22145
3.10E-01	8.16163
3.57E-01	8.85561
3.98E-01	10.2576
4.39E-01	13.0743
4.72E-01	18.0276
5.05E-01	22.5982
5.50E-01	18.1696
5.94E-01	14.5444
6.42E-01	12.7458
6.89E-01	12.006
7.37E-01	11.4059
7.85E-01	10.5542
8.34E-01	9.80179
8.83E-01	9.05816
9.32E-01	8.40416
9.82E-01	7.74431
1.03109	7.17942
1.08067	6.61148

Table B- 9 Abaqus analysis results for the study investigating effect of end plate thickness and mast arm outer diameter on SCF at weld toe-11 in mast arm diameter

1 in		1.25 inches		1.5 inches		2 inches		2.5 inches		3 inches	
Distance from face of end plate (in)	Max. Principal stress (ksi)	Distance from face of end plate (in)	Max. Principal stress (ksi)	Distance from face of end plate (in)	Max. Principal stress (ksi)	Distance from face of end plate (in)	Max. Principal stress (ksi)	Distance from face of end plate (in)	Max. Principal stress (ksi)	Distance from face of end plate (in)	Max. Principal stress (ksi)
0	19.3551	0	14.33	0	10.72	0	6.45646	0	4.19834	0	2.97389
7.71E-02	24.4709	7.71E-02	18.0261	7.71E-02	13.6019	7.71E-02	8.46954	7.71E-02	5.90614	7.71E-02	4.5149
1.54E-01	22.506	1.54E-01	17.1674	1.54E-01	13.5881	1.54E-01	9.6273	1.54E-01	7.74698	1.54E-01	6.755
2.10E-01	22.2352	2.10E-01	17.5039	2.10E-01	14.2849	2.10E-01	10.7954	2.10E-01	9.18769	2.10E-01	8.35876
2.66E-01	23.023	2.66E-01	18.6857	2.66E-01	15.5465	2.66E-01	12.0954	2.66E-01	10.4938	2.66E-01	9.66339
3.13E-01	24.9502	3.13E-01	20.7799	3.13E-01	17.5834	3.13E-01	14.0088	3.13E-01	12.3283	3.13E-01	11.4482
3.61E-01	26.5077	3.61E-01	22.3853	3.61E-01	19.113	3.61E-01	15.4178	3.61E-01	13.6676	3.61E-01	12.7458
4.01E-01	29.819	4.01E-01	25.5487	4.01E-01	22.0928	4.01E-01	18.1755	4.01E-01	16.3166	4.01E-01	15.3362
4.42E-01	37.2345	4.42E-01	32.3501	4.42E-01	28.3334	4.42E-01	23.7784	4.42E-01	21.6212	4.42E-01	20.4853
4.74E-01	49.5431	4.74E-01	43.6382	4.74E-01	38.7363	4.74E-01	33.1958	4.74E-01	30.5875	4.74E-01	29.2209
5.05E-01	**59.4242**	**5.05E-01**	**52.9571**	**5.05E-01**	**47.538**	**5.05E-01**	**41.4399**	**5.05E-01**	**38.591**	**5.05E-01**	**37.1075**
5.53E-01	46.3571	5.53E-01	41.6475	5.53E-01	37.6908	5.53E-01	33.2764	5.53E-01	31.24	5.53E-01	30.1904
6.01E-01	36.4943	6.01E-01	33.0189	6.01E-01	30.097	6.01E-01	26.8725	6.01E-01	25.4087	6.01E-01	24.6644
6.50E-01	31.4887	6.50E-01	28.6793	6.50E-01	26.3131	6.50E-01	23.7304	6.50E-01	22.5774	6.50E-01	21.9998
6.99E-01	29.1872	6.99E-01	26.7485	6.99E-01	24.6895	6.99E-01	22.4681	6.99E-01	21.4946	6.99E-01	21.015
7.48E-01	27.2483	7.48E-01	25.1368	7.48E-01	23.3446	7.48E-01	21.434	7.48E-01	20.6133	7.48E-01	20.2167
7.97E-01	24.6573	7.97E-01	22.9485	7.97E-01	21.486	7.97E-01	19.9573	7.97E-01	19.323	7.97E-01	19.0269
8.47E-01	22.4092	8.47E-01	21.0566	8.47E-01	19.8827	8.47E-01	18.6852	8.47E-01	18.2111	8.47E-01	18.0008
8.96E-01	20.1932	8.96E-01	19.1938	8.96E-01	18.3057	8.96E-01	17.4363	8.96E-01	17.1207	8.96E-01	16.9953
9.46E-01	18.2862	9.46E-01	17.5957	9.46E-01	16.955	9.46E-01	16.367	9.46E-01	16.186	9.46E-01	16.1322
9.96E-01	16.3613	9.96E-01	15.9823	9.96E-01	15.5909	9.96E-01	15.2863	9.96E-01	15.2408	9.96E-01	15.259
1.04523	14.7431	1.04523	14.631	1.04523	14.4509	1.04523	14.384	1.04523	14.4509	1.04523	14.5282
1.09489	13.1169	1.09489	13.2729	1.09489	13.3048	1.09489	13.4767	1.09489	13.6563	1.09489	13.793

Table B- 10 Abaqus analysis results for the study investigating effect of mast arm outer diameter on SCF at weld toe – 6.5 in mast arm diameter

1 inch		1.25 inches		1.5 inches		2 inches		2.5 inches		3 inches	
Distance from face of end plate (in)	Max. Principal stress (ksi)	Distance from face of end plate (in)	Max. Principal stress (ksi)	Distance from face of end plate (in)	Max. Principal stress (ksi)	Distance from face of end plate (in)	Max. Principal stress (ksi)	Distance from face of end plate (in)	Max. Principal stress (ksi)	Distance from face of end plate (in)	Max. Principal stress (ksi)
0	59.5171	0	47.6861	0	37.7178	0	24.9966	0	17.8074	0	13.9924
9.02E-02	69.0879	9.02E-02	55.3952	9.02E-02	44.399	7.69E-02	31.4097	9.02E-02	24.0552	7.69E-02	19.927
1.80E-01	58.5705	1.80E-01	48.4594	1.80E-01	40.4636	1.54E-01	30.5459	1.80E-01	26.701	1.54E-01	22.9723
2.47E-01	56.7456	2.47E-01	48.8516	2.47E-01	42.1433	2.09E-01	31.6657	2.47E-01	30.7469	2.09E-01	25.7609
3.14E-01	59.0647	3.14E-01	52.6707	3.14E-01	46.2776	2.65E-01	35.1892	3.14E-01	34.8365	2.65E-01	29.4356
3.67E-01	66.0199	3.67E-01	60.4635	3.67E-01	54.0751	3.11E-01	40.5217	3.67E-01	42.1822	3.11E-01	34.5547
4.20E-01	79.0924	4.20E-01	73.8013	4.20E-01	67.0062	3.58E-01	44.3012	4.20E-01	54.1233	3.58E-01	38.1819
4.63E-01	106.581	4.63E-01	101.285	4.63E-01	93.5957	3.98E-01	51.4583	4.63E-01	78.8828	3.98E-01	45.1279
5.05E-01	**136.127**	**5.05E-01**	**131.423**	**5.05E-01**	**123.241**	4.39E-01	65.6247	**5.05E-01**	**107.439**	4.39E-01	58.6206
5.50E-01	106.964	5.50E-01	104.378	5.50E-01	98.8983	4.72E-01	91.3797	5.50E-01	88.3374	4.72E-01	83.3072
5.96E-01	80.8936	5.96E-01	79.7442	5.96E-01	76.2978	**5.05E-01**	**114.649**	5.96E-01	69.6976	**5.05E-01**	**106.254**
6.43E-01	67.7183	6.43E-01	67.4125	6.43E-01	65.0902	5.51E-01	90.8752	6.43E-01	60.6719	5.51E-01	85.4215
6.91E-01	61.1841	6.91E-01	61.4998	6.91E-01	59.9055	5.97E-01	71.6517	6.91E-01	56.9002	5.97E-01	68.2624
7.39E-01	56.1402	7.39E-01	56.9833	7.39E-01	55.9815	6.45E-01	62.0005	7.39E-01	54.1054	6.45E-01	59.767
7.88E-01	49.4395	7.88E-01	50.8809	7.88E-01	50.5825	6.92E-01	57.7453	7.88E-01	50.0484	6.92E-01	56.2695
8.37E-01	43.9971	8.37E-01	45.9407	8.37E-01	46.2191	7.41E-01	54.5428	8.37E-01	46.7674	7.41E-01	53.6655
8.86E-01	38.6108	8.86E-01	41.0547	8.86E-01	41.907	7.89E-01	50.0568	8.86E-01	43.5312	7.89E-01	49.886
9.36E-01	34.3285	9.36E-01	37.1816	9.36E-01	38.4923	8.38E-01	46.4322	9.36E-01	40.9596	8.38E-01	46.8243
9.85E-01	30.0114	9.85E-01	33.2752	9.85E-01	35.0469	8.87E-01	42.8548	9.85E-01	38.3614	8.87E-01	43.806
1.03514	26.7188	1.03514	30.3081	1.03514	32.4344	9.37E-01	40.0212	1.03514	36.3852	9.37E-01	41.4042
1.0848	23.4172	1.0848	27.3319	1.0848	29.8134	9.86E-01	37.1597	1.0848	34.4006	9.86E-01	38.9764

Table B- 11 Abaqus analysis results for the study investigating the effect of weld dimensions on SCF at weld toe – 7q weld for 0.179 thick mast arm

1 inch		1.25 inches		1.5 inches		2 inches		2.5 inches		3 inches	
Distance from face of end plate (in)	Max. Principal stress (ksi)	Distance from face of end plate (in)	Max. Principal stress (ksi)	Distance from face of end plate (in)	Max. Principal stress (ksi)	Distance from face of end plate (in)	Max. Principal stress (ksi)	Distance from face of end plate (in)	Max. Principal stress (ksi)	Distance from face of end plate (in)	Max. Principal stress (ksi)
0	28.6569	0	19.5129	0	13.9198	0	8.17096	0	5.16381	0	3.43832
1.01E-01	36.3445	1.01E-01	25.7042	1.01E-01	19.1858	1.01E-01	12.3712	1.01E-01	9.25085	1.01E-01	7.63887
2.01E-01	36.4655	2.01E-01	28.4422	2.01E-01	23.291	2.01E-01	17.9784	2.01E-01	15.6117	2.01E-01	14.4076
2.83E-01	56.1743	2.83E-01	47.5777	2.83E-01	41.5914	2.83E-01	35.2292	2.83E-01	32.3148	2.83E-01	30.7956
3.65E-01	**90.4662**	**3.65E-01**	**79.4608**	**3.65E-01**	**71.5571**	**3.65E-01**	**63.1029**	**3.65E-01**	**59.2151**	**3.65E-01**	**57.1818**
4.56E-01	67.1011	4.56E-01	60.0904	4.56E-01	55.0581	4.56E-01	49.7376	4.56E-01	47.3291	4.56E-01	46.0848
5.46E-01	48.8785	5.46E-01	44.638	5.46E-01	41.6087	5.46E-01	38.4873	5.46E-01	37.123	5.46E-01	36.4379
6.36E-01	41.3321	6.36E-01	38.458	6.36E-01	36.3967	6.36E-01	34.3319	6.36E-01	33.4667	6.36E-01	33.0482
7.26E-01	32.9765	7.26E-01	31.5668	7.26E-01	30.542	7.26E-01	29.6019	7.26E-01	29.2645	7.26E-01	29.1263
8.16E-01	27.0571	8.16E-01	26.7163	8.16E-01	26.4327	8.16E-01	26.282	8.16E-01	26.3075	8.16E-01	26.3592
9.06E-01	21.0005	9.06E-01	21.7324	9.06E-01	22.1935	9.06E-01	22.8355	9.06E-01	23.2249	9.06E-01	23.4668
9.96E-01	16.9783	9.96E-01	18.445	9.96E-01	19.4045	9.96E-01	20.5656	9.96E-01	21.1872	9.96E-01	21.5481
1.08662	13.2414	1.08664	15.3955	1.08662	16.8202	1.08662	18.4636	1.08662	19.2994	1.08662	19.7695
1.17678	11.0217	1.17679	13.6056	1.17678	15.3096	1.17678	17.2315	1.17678	18.1851	1.17678	18.7129
1.26693	8.94144	1.26695	11.9264	1.26693	13.8907	1.26693	16.0705	1.26693	17.1319	1.26693	17.7119
1.35708	7.9529	1.3571	11.147	1.35708	13.2367	1.35708	15.5295	1.35708	16.6317	1.35708	17.2288
1.44724	7.10374	1.44725	10.4822	1.44724	12.6798	1.44724	15.0664	1.44724	16.2002	1.44724	16.8092
1.53739	6.96749	1.53741	10.3991	1.53739	12.6152	1.53739	15.0022	1.53739	16.1256	1.53739	16.725
1.62754	6.9359	1.62756	10.4024	1.62754	12.6238	1.62754	14.9967	1.62754	16.1027	1.62754	16.6887
1.7177	7.31939	1.71772	10.7402	1.7177	12.9142	1.7177	15.2199	1.7177	16.2858	1.7177	16.8471
1.80785	7.78524	1.80787	11.1458	1.80785	13.2621	1.80785	15.4891	1.80785	16.5097	1.80785	17.0434
1.89801	8.44327	1.89803	11.7027	1.89801	13.7362	1.89801	15.8614	1.89801	16.8277	1.89801	17.33
1.98816	9.16177	1.98818	12.309	1.98816	14.2518	1.98816	16.2668	1.98816	17.1749	1.98816	17.6438

APPENDIX C

Table C- 1 Abaqus analysis results for the study investigating the effect of weld orientation on stresses at weld toe

Long leg on mast arm		Equal legs		Long leg on end plate	
Distance from face of end plate (in)	Max. Principal stress (ksi)	Distance from face of end plate (in)	Max. Principal stress (ksi)	Distance from face of end plate (in)	Max. Principal stress (ksi)
0	14.44	0	9.9979	0	9.62282
1.38E-01	17.2194	1.34E-01	10.9977	8.79E-02	10.4114
2.76E-01	16.9654	2.68E-01	11.7507	1.76E-01	10.6816
3.91E-01	26.1043	3.66E-01	13.0364	2.37E-01	11.673
5.06E-01	**40.2839**	4.64E-01	14.1718	2.98E-01	12.5062
6.22E-01	29.7994	5.43E-01	27.0556	3.47E-01	12.7133
7.38E-01	21.3676	**6.22E-01**	**52.9074**	3.97E-01	17.452
8.56E-01	17.2753	7.43E-01	32.6045	4.52E-01	32.8641
9.74E-01	13.3691	8.64E-01	22.1161	**5.06E-01**	**44.0356**
1.09419	10.7425	9.84E-01	19.0124	6.26E-01	34.7372
1.21389	8.06711	1.10469	14.3851	7.45E-01	24.2681
1.33424	6.46599	1.22526	11.4713	8.65E-01	20.5346
1.45458	5.03148	1.34582	8.59113	9.84E-01	16.0436
1.57527	4.34084	1.46639	6.83109	1.10328	12.6974
1.69596	3.72741	1.58696	5.23384	1.22264	9.54045
1.81684	3.59712	1.70753	4.44302	1.34201	7.60021
1.93772	3.5371	1.82809	3.7455	1.46138	5.78562
2.0587	3.7429	1.94866	3.56233	1.58075	4.82246
2.17969	3.99666	2.06923	3.45829	1.70012	3.94318
2.30073	4.36175	2.18979	3.64211	1.81948	3.6479
2.42177	4.76046	2.31036	3.88108	1.93884	3.41735
2.54288	5.16997	2.43093	4.2445	2.05819	3.52772
2.66398	5.60022	2.5515	4.64601	2.17755	3.68597
2.78508	5.98395	2.67206	5.06559	2.2969	4.00852
2.90617	6.3788	2.79263	5.50845	2.41626	4.36627
3.02727	6.7013	2.9132	5.90811	2.53561	4.76735
3.14836	7.02799	3.03376	6.32003	2.65496	5.19402

APPENDIX D

Results obtained from the Abaqus analysis to be used for calculating SCF using DONG's Structural Stress approach are given in this section. The following tables give the distance of points through the mast arm thickness for a section located at weld toe and the value of normal stress at those points ($\sigma_x(y)$). From these values, a graph is drawn and using Equations 3.5 and 3.6, membrane and bending components of structural stress are calculated. Structural stress at the critical section is calculated using Equation 3.4 and the resulting value is substituted in the numerator of Equation 3.1 to determine the SCF at weld toe.

Table D- 1 Abaqus analysis results for Mesh Convergence study using DONG's Structural Stress approach-Specimen 'A'

0.1 inch		0.15 inch		0.2 inch	
Distance through thickness of mast arm (in)	Normal stress $\sigma_x(y)$	Distance through thickness of mast arm (in)	Normal stress $\sigma_x(y)$	Distance through thickness of mast arm (in)	Normal stress $\sigma_x(y)$
0	-15.4632	0	-14.4159	0	-14.3639
3.24E-02	5.28016	3.91E-02	8.97011	3.63E-02	7.64321
6.49E-02	23.5824	7.83E-02	31.251	7.27E-02	28.6405
9.53E-02	38.0912	1.09E-01	49.6836	1.03E-01	46.713
1.26E-01	57.4791	1.39E-01	69.1298	1.33E-01	65.3572
1.52E-01	89.084	1.59E-01	93.9333	1.56E-01	90.8954
1.79E-01	139.876	1.79E-01	121.643	1.79E-01	119.329

Table D- 2 Abaqus analysis results for Mesh Convergence study using DONG's Structural Stress approach-Specimen 'B'

0.1 inch		0.15 inch		0.2 inch	
Distance through thickness of mast arm (in)	Normal stress $\sigma_x(y)$	Distance through thickness of mast arm (in)	Normal stress $\sigma_x(y)$	Distance through thickness of mast arm (in)	Normal stress $\sigma_x(y)$
0	-24.7603	0	-24.5068	0	-24.6059
4.32E-02	-5.89675	4.52E-02	-5.35507	4.59E-02	-5.31381
8.64E-02	10.8077	9.03E-02	12.131	9.18E-02	12.5368
1.27E-01	24.0544	1.31E-01	27.01	1.33E-01	28.2277
1.68E-01	41.93	1.72E-01	45.1576	1.74E-01	46.6393
2.04E-01	70.6529	2.06E-01	72.7037	2.07E-01	72.9793
2.41E-01	116.349	2.40E-01	109.359	2.41E-01	107.613

Table D- 3 Abaqus analysis results for TXu and VALu specimens

Txu		VALu	
Distance through thickness of mast arm (in)	Normal stress $\sigma_x(y)$	Distance through thickness of mast arm (in)	Normal stress $\sigma_x(y)$
0	-16.2147	0	-20.614
4.45E-02	-7.54471	3.25E-02	-9.20333
8.90E-02	2.72E-01	6.50E-02	1.04148
1.28E-01	6.11484	9.54E-02	9.50562
1.68E-01	13.8367	1.26E-01	20.1055
2.04E-01	25.5	1.52E-01	35.5915
2.40E-01	45.1007	1.79E-01	59.5766

Table D- 4 Abaqus analysis results for VALNu and VALNu2 specimens

VALNu		VALNu2	
Distance through thickness of mast arm (in)	Normal stress $\sigma_x(y)$	Distance through thickness of mast arm (in)	Normal stress $\sigma_x(y)$
0	-20.6229	0	-11.7319
3.25E-02	-9.20731	3.48E-02	-2.52321
6.50E-02	1.04191	6.96E-02	5.90913
9.54E-02	9.5097	9.99E-02	12.8091
1.26E-01	20.1142	1.30E-01	21.2915
1.52E-01	35.6068	1.55E-01	33.5115
1.79E-01	59.6023	1.79E-01	49.4703

Table D- 5 Abaqus analysis results for Nippon steel specimens

Nippon steel A		Nippon steel B	
Distance through thickness of mast arm (in)	Normal stress $\sigma_x(y)$	Distance through thickness of mast arm (in)	Normal stress $\sigma_x(y)$
0	-13.1123	0	-6.25856
3.25E-02	-3.70889	4.44E-02	-2.41736
6.50E-02	4.69926	8.89E-02	1.06545
9.54E-02	11.517	1.28E-01	3.62321
1.26E-01	20.2616	1.68E-01	7.07337
1.53E-01	33.5654	2.04E-01	12.384
1.79E-01	54.5021	2.40E-01	21.425

Table D- 6 Abaqus analysis results for the study investigating effect of end plate thickness and mast arm outer diameter on SCF at weld toe – 11 in mast arm diameter

1 inch		1.25 inches		1.5 inches		2 inches		2.5 inches		3 inches	
Distance through thickness of mast arm (in)	Normal stress $\sigma_x(y)$	Distance through thickness of mast arm (in)	Normal stress $\sigma_x(y)$	Distance through thickness of mast arm (in)	Normal stress $\sigma_x(y)$	Distance through thickness of mast arm (in)	Normal stress $\sigma_x(y)$	Distance through thickness of mast arm (in)	Normal stress $\sigma_x(y)$	Distance through thickness of mast arm (in)	Normal stress $\sigma_x(y)$
0	-25.0225	0	-18.0425	0	-12.7725	0	-6.90058	0	-4.14706	0	-2.70869
4.45E-02	-13.0645	4.45E-02	-8.17438	4.45E-02	-4.53527	4.45E-02	-4.79E-01	4.45E-02	1.4293	4.45E-02	2.42855
8.89E-02	-2.3521	8.89E-02	6.49E-01	8.89E-02	2.81053	8.89E-02	5.22129	8.89E-02	6.36309	8.89E-02	6.96426
1.25E-01	5.06208	1.25E-01	6.65917	1.25E-01	7.72596	1.25E-01	8.91457	1.25E-01	9.48483	1.25E-01	9.78812
1.62E-01	14.6719	1.62E-01	14.6132	1.62E-01	14.378	1.62E-01	14.1129	1.62E-01	14.0045	1.62E-01	13.9545
2.01E-01	30.3098	2.01E-01	27.8798	2.01E-01	25.7443	2.01E-01	23.3466	2.01E-01	22.2384	2.01E-01	21.6662
2.39E-01	56.5042	2.39E-01	50.4044	2.39E-01	45.2901	2.39E-01	39.539	2.39E-01	36.855	2.39E-01	35.4584

Table D- 7 Abaqus analysis results for the study investigating effect of end plate thickness and mast arm outer diameter on SCF at weld toe – 6.5 in mast arm diameter

1 inch		1.25 inches		1.5 inches		2 inches		2.5 inches		3 inches	
Distance through thickness of mast arm (in)	Normal stress $\sigma_x(y)$	Distance through thickness of mast arm (in)	Normal stress $\sigma_x(y)$	Distance through thickness of mast arm (in)	Normal stress $\sigma_x(y)$	Distance through thickness of mast arm (in)	Normal stress $\sigma_x(y)$	Distance through thickness of mast arm (in)	Normal stress $\sigma_x(y)$	Distance through thickness of mast arm (in)	Normal stress $\sigma_x(y)$
0	-45.8054	0	-34.7783	0	-24.7501	0	-12.9479	0	-7.20651	0	-4.26792
4.32E-02	-21.6541	4.32E-02	-13.184	4.32E-02	-5.89155	4.50E-02	3.27565	4.32E-02	6.74385	4.50E-02	9.38734
8.64E-02	-2.43E-01	8.64E-02	5.96283	8.64E-02	10.8084	9.01E-02	17.7329	8.64E-02	19.0412	9.01E-02	21.5437
1.27E-01	17.2006	1.27E-01	21.3648	1.27E-01	24.0515	1.28E-01	27.2597	1.27E-01	28.3958	1.28E-01	29.2819
1.68E-01	39.804	1.68E-01	41.7186	1.68E-01	41.9223	1.65E-01	40.8266	1.68E-01	41.7752	1.65E-01	40.7674
2.04E-01	74.2614	2.04E-01	73.5912	2.04E-01	70.6382	2.02E-01	65.2664	2.04E-01	64.6504	2.02E-01	62.2034
2.41E-01	128.171	2.41E-01	123.899	2.41E-01	116.323	2.40E-01	108.813	2.41E-01	101.687	2.40E-01	101.008

References

1. Koenigs, Mark T.; Botros, Tamer A.; Freytag, Dylan; and Frank, Karl H. Research Report 0-4178-2: Fatigue Strength of Signal Mast Arm Connections. Center for Transportation Research, Bureau of Engineering Research, The University of Texas at Austin, August 2003.

2. Dexter, R. J., and Ricker, M. J. Fatigue-Resistant Design of Cantilevered Signal, Sign and Light Supports. NCHRP, TRB, National Research Council, Washington, D.C., June 2001.

3. Kaczinski, M. R.; Dexter R. J.; and Van Dien, J. P. NCHRP Report 412: Fatigue Resistant Design of Cantilevered Signal, Sign and Light Supports. TRB, National Research Council, Washington, D.C., 1998.

4. Palmatier, Amanda H., Ultrasonic Impact Treatment of Traffic Signal Mast Arm Welds. Masters of Science in Engineering Thesis, The University of Texas at Austin, May, 2005.

5. Dong P., A Structural stress definition and numerical implementation for fatigue analysis of welded joints. International Journal of Fatigue 23 (2001) 865-876, June 2001.

6. Guidelines for the Installation, Inspection, Maintenance and Repair of Structural Supports for Highway Signs, Luminaries, and Traffic Signals. U. S. Department of Transportation, Federal Highway Administration, Bridge Technology, November 2005.

7. Puckett, J. A.; Hamilton, H. R.; Collins, B. P.; Huck, P. Traffic Signal Pole Fatigue in Wyoming – A Research Overview. University of Wyoming and Wyoming Department of Transportation.

8. Hibbit; Karlson; and Sorenson. Abaqus/Standard/ Users Manual. Version 6.1. Pawtucket, Rhode Island. 2000.

9. Analysis User's Manual-Volume I: Introduction, Spatial Modeling, Execution and Output – Abaqus version 6.5.

10. Example Problems Manual – Abaqus version 6.5.

11. Florea, Micah J., Field Tests and Analytical Studies of the Dynamic Behavior and the Onset of Galloping in Traffic Signal Structures. Masters of Science in Engineering thesis, The University of Texas at Austin, May 2005.

12. Hall III, John H., The Effect of Baseplate Flexibility on the Fatigue Performance of Welded Socket Connections in Cantilevered Sign Structures. Masters of Science in Engineering thesis, Lehigh University, January 2005.

13. Koenigs, M. T. K. Fatigue Resistance of Traffic Signal Mast-Arm Connection Details. Masters of Science in Engineering Thesis, The University of Texas at Austin, May, 2003.

14. Barsom, John M. and Rolfe, Stanley T. Fracture and Fatigue Control in Structures. Second Edition. Englewood Cliffs, New Jersey: Prentice Hall, 1987.

15. Field and Laboratory Fatigue Investigation and Inspection of Cantilevered Mast-arm Signal Support Structures. Advanced Technology for Large Structural Systems: A National Engineering Research Center, Lehigh University

VITA

Ramadevi Duraisamy was born on February 28, 1982 in Madurai, Tamilnadu, India, the daughter of Duraisamy Ramamoorthy and Rajeshwari Duraisamy. After completing her work at DAV Senior Secondary School, Chennai, Tamilnadu, India in 1999, she began her undergraduate study at the Regional Engineering College Trichy, Tamilnadu, India and graduated in 2003 with a Bachelor of Civil Engineering degree. In August 2004, she began her graduate study in the Structural Engineering program at The University of Texas at Austin in pursuit of a Master of Science in Engineering degree. During her stay at the university, she worked as a grader and as a student intern at The University of Texas at Austin, Physical plant.

Permanent Address: 172/12 Golden Jubilee Flats

Annanagar West, Chennai 600040

ramaduraisamy@hotmail.com

This thesis was typed by the author.